Biallelic Mutations in *MRPS34* Lead to Instability of the Small Mitoribosomal Subunit and Leigh Syndrome

Nicole J. Lake,[1,2,23] Bryn D. Webb,[3,4,5,23] David A. Stroud,[6,23] Tara R. Richman,[7,23] Benedetta Ruzzenente,[8] Alison G. Compton,[1,2] Hayley S. Mountford,[1,2,9] Juliette Pulman,[8] Coralie Zangarelli,[8] Marlene Rio,[10] Nathalie Bodaert,[11] Zahra Assouline,[10] Mingma D. Sherpa,[3,5] Eric E. Schadt,[3,5] Sander M. Houten,[3,5] James Byrnes,[12] Elizabeth M. McCormick,[12] Zarazuela Zolkipli-Cunningham,[12,13] Katrina Haude,[14] Zhancheng Zhang,[14] Kyle Retterer,[14] Renkui Bai,[14] Sarah E. Calvo,[15,16,17] Vamsi K. Mootha,[15,16,17] John Christodoulou,[1,2] Agnes Rötig,[8] Aleksandra Filipovska,[7,18] Ingrid Cristian,[19,20] Marni J. Falk,[12,21,24] Metodi D. Metodiev,[8,24] and David R. Thorburn[1,2,22,24,*]

The synthesis of all 13 mitochondrial DNA (mtDNA)-encoded protein subunits of the human oxidative phosphorylation (OXPHOS) system is carried out by mitochondrial ribosomes (mitoribosomes). Defects in the stability of mitoribosomal proteins or mitoribosome assembly impair mitochondrial protein translation, causing combined OXPHOS enzyme deficiency and clinical disease. Here we report four autosomal-recessive pathogenic mutations in the gene encoding the small mitoribosomal subunit protein, MRPS34, in six subjects from four unrelated families with Leigh syndrome and combined OXPHOS defects. Whole-exome sequencing was used to independently identify all variants. Two splice-site mutations were identified, including homozygous c.321+1G>T in a subject of Italian ancestry and homozygous c.322−10G>A in affected sibling pairs from two unrelated families of Puerto Rican descent. In addition, compound heterozygous *MRPS34* mutations were identified in a proband of French ancestry; a missense (c.37G>A [p.Glu13Lys]) and a nonsense (c.94C>T [p.Gln32*]) variant. We demonstrated that these mutations reduce MRPS34 protein levels and the synthesis of OXPHOS subunits encoded by mtDNA. Examination of the mitoribosome profile and quantitative proteomics showed that the mitochondrial translation defect was caused by destabilization of the small mitoribosomal subunit and impaired monosome assembly. Lentiviral-mediated expression of wild-type *MRPS34* rescued the defect in mitochondrial translation observed in skin fibroblasts from affected subjects, confirming the pathogenicity of *MRPS34* mutations. Our data establish that MRPS34 is required for normal function of the mitoribosome in humans and furthermore demonstrate the power of quantitative proteomic analysis to identify signatures of defects in specific cellular pathways in fibroblasts from subjects with inherited disease.

Introduction

The oxidative phosphorylation (OXPHOS) system generates the majority of cellular energy required by the body. Mitochondrial DNA (mtDNA) encodes 13 protein subunits of the OXPHOS system via 11 mRNAs, 2 of which are bicistronic (*MT-ATP8/MT-ATP6* and *MT-ND4L/MT-ND4*), as well as 22 transfer RNAs (mt-tRNA) required for translation and 2 ribosomal RNAs (mt-rRNA) necessary for the assembly of mitochondrial ribosomes (mitoribosomes). Nuclear genes encode all of the other proteins required for mitochondrial translation, including mitoribosomal proteins, tRNA- and rRNA-modifying enzymes, and additional factors that mediate mitoribosome biogenesis and translation initiation, elongation, and termination.[1]

Mammalian mitoribosomes contain two subunits: a small (28S) subunit that decodes mRNA and mediates tRNA delivery of required amino acids and a large (39S)

[1]Murdoch Children's Research Institute, Royal Children's Hospital, Melbourne, VIC 3052, Australia; [2]Department of Paediatrics, University of Melbourne, Melbourne, VIC 3052, Australia; [3]Department of Genetics and Genomic Sciences, Icahn School of Medicine at Mount Sinai, New York, NY 10029, USA; [4]Department of Pediatrics, Icahn School of Medicine at Mount Sinai, New York, NY 10029, USA; [5]Icahn Institute for Genomics and Multiscale Biology, Icahn School of Medicine at Mount Sinai, New York, NY 10029, USA; [6]Department of Biochemistry and Molecular Biology, Monash Biomedicine Discovery Institute, Monash University, Clayton Campus, Melbourne, VIC 3800, Australia; [7]Harry Perkins Institute of Medical Research and Centre for Medical Research, University of Western Australia, Nedlands, WA 6009, Australia; [8]INSERM U1163, Université Paris Descartes - Sorbonne Paris Cité, Institut Imagine, 75015 Paris, France; [9]Department of Biological and Medical Sciences, Faculty of Health Sciences, Oxford Brookes University, Oxford OX3 0BP, UK; [10]Departments of Pediatric, Neurology and Genetics, Hôpital Necker-Enfants-Malades, 75015 Paris, France; [11]Pediatric Radiology Department, Hôpital Necker Enfants Malades, AP-HP, University René Descartes, PRES Sorbonne Paris Cité, INSERM U1000 and UMR 1163, Institut Imagine, 75015 Paris, France; [12]Division of Human Genetics, Department of Pediatrics, The Children's Hospital of Philadelphia, Philadelphia, PA 19104, USA; [13]Division of Neurology, Department of Pediatrics, The Children's Hospital of Philadelphia, Philadelphia, PA 19104, USA; [14]GeneDx, Gaithersburg, MD 20877, USA; [15]Howard Hughes Medical Institute, Department of Molecular Biology, Massachusetts General Hospital, Boston, MA 02114, USA; [16]Department of Systems Biology, Harvard Medical School, Boston, MA 02115, USA; [17]Broad Institute of MIT and Harvard, Cambridge, MA 02142, USA; [18]School of Molecular Sciences, University of Western Australia, Crawley, WA 6009, Australia; [19]Nemours Children's Hospital, Orlando, FL 32827, USA; [20]Division of Genetics, Arnold Palmer Hospital for Children, Orlando, FL 32806, USA; [21]University of Pennsylvania Perelman School of Medicine, Philadelphia, PA 19104, USA; [22]Victorian Clinical Genetic Services, Royal Children's Hospital, Melbourne, VIC 3052, Australia
[23]These authors contributed equally to this work
[24]These authors contributed equally to this work
*Correspondence: david.thorburn@mcri.edu.au
http://dx.doi.org/10.1016/j.ajhg.2017.07.005.

subunit that catalyzes the formation of peptide bonds between the amino acids.[2,3] In humans, 30 mitochondrial ribosomal small subunit proteins (MRPSs) assemble with the 12S mt-rRNA to form the small 28S subunit, while 50 mitochondrial ribosomal large subunit proteins (MRPLs) assemble with the 16S mt-rRNA and mt-tRNA^{Val} to form the large 39S subunit.[4–6]

Molecular defects that impair different components of the mitochondrial translation machinery can cause combined OXPHOS deficiency.[7] Specifically, 7 of the 80 genes encoding mitochondrial ribosomal proteins have had pathogenic mutations reported, including autosomal-recessive mutations in *MRPS7* (MIM: 611974),[8] *MRPS16* (MIM: 609204),[9] *MRPS22* (MIM: 605810),[10] *MRPS23* (MIM: 611985),[11] *MRPL3* (MIM: 607118),[12] *MRPL12* (MIM: 602375),[13] and *MRPL44* (MIM: 611849).[14] Disorders caused by mutations in mitoribosomal proteins are clinically heterogeneous and multi-systemic, with common features including neurodevelopmental disabilities, brain abnormalities, liver disease, kidney disease, cardiomyopathy, and lactic acidosis.[11,15] They generally lead to death in infancy or early childhood,[15] although survival into teenage years and adulthood has been reported.[8,14,16] The small number of mitoribosomal genes known to underlie OXPHOS diseases is surprising, since nearly two-thirds of mitoribosomal genes are essential for OXPHOS based on a high-throughput knock-out death screen in cell models.[17]

Here, we report four pathogenic recessive mutations in a small mitoribosome subunit gene, *MRPS34*, not previously associated with human disease that were identified in six individuals from four families with combined OXPHOS defects and Leigh syndrome or Leigh-like disease (MIM: 256000). MRPS34, which lies within the foot of the small 28S mitoribosome subunit, is one of 15 mammalian mitochondria-specific MRPSs not found in the ancestral bacterial ribosome.[5] We previously showed that mice with a homozygous *Mrps34* missense mutation that caused reduced MRPS34 protein stability developed cardiac hypertrophy and pronounced liver dysfunction due to impaired mitoribosome assembly.[18] We now demonstrate that human *MRPS34* mutations cause Leigh or Leigh-like syndrome by destabilizing the small mitoribosomal subunit and impairing mitochondrial protein translation.

Subjects and Methods

Samples from probands and family members were obtained after receiving informed consent for diagnostic or research investigations, and associated studies were performed in accordance with the Declaration of Helsinki and approved by the respective human research institutional review board responsible for each research site.

Clinical Information

A summary of features in the six affected subjects from four unrelated families is shown in Table 1, with detailed descriptions provided in the Supplemental Note and Table S1. Most subjects had normal neonatal periods, with subsequent onset of developmental delay in all patients by 6 months of age that typically evolved to neurodevelopmental regression. Subjects 1 and 4 had failure to thrive in the first few months of life and episodic metabolic acidosis with respiratory distress, with death during an episode between 8 to 9 months of age. They had progressive clinical courses with brain MRI and/or neuropathology analysis showing lesions in the basal ganglia, brainstem, and/or midbrain that were diagnostic of the progressive neurodegenerative disorder Leigh syndrome (Figure S1 for subject 4 MRI).[19] Similar but milder clinical courses typical of Leigh or Leigh-like syndrome have been seen in subjects 2a, 2b, 3a, and 3b, with all still alive at ages ranging from 2 to 17 years. The subject with Leigh-like syndrome had neuroradiological imaging that did not fulfil stringent diagnostic criteria for Leigh syndrome.[19] The three older subjects have developed dystonic and/or choreoathetoid movements, with wheelchair dependence. Four of the subjects had OXPHOS enzymology performed in skeletal muscle, liver, and/or skin fibroblast cell lines, which showed deficiency of one or more OXPHOS complexes (Tables 1 and S2).

Enzyme Assays

Spectrophotometric enzyme assays assessing mitochondrial OXPHOS enzyme and citrate synthase activities in cultured fibroblasts, skeletal muscle, and liver biopsy were performed as described previously for subjects 1 and 4.[20,21] For subject 2a, clinical skeletal muscle OXPHOS enzymology testing was performed at 19 months at All Children's Hospital (St. Petersburg, FL, USA) and at 12 years at MNG Laboratories (Atlanta, GA, USA). Enzyme studies for subject 3a were performed at Baylor Medical Genetics Laboratory. Dipstick assays to measure complexes I and IV activity in lentiviral rescue studies were performed on 15 μg of fibroblast lysates as described previously.[22]

Whole-Exome Sequencing

Whole-exome sequencing (WES) of subject 1 was performed at the Broad Institute using Illumina Capture Exome technology (version 1) supplemented with additional baits to ensure capture of mtDNA. Data were mapped to NCBI hg19/GRCh37 human genome reference sequence using BWA,[23] and then analyzed using GATK Best Practices recommendations,[24] HaplotypeCaller,[25,26] Variant Effect Predictor,[27] and Seqr. Analysis of mtDNA was performed as described previously.[28]

Clinical WES testing was performed for subjects 2a, 2b, and 3a and their parents as described.[29] DNA libraries were generated using the SureSelect Human All Exon V4 or Clinical Research Exome kit (Agilent Technologies). Data were mapped to the NCBI hg19/GRCh37 human genome reference sequence and analyzed using GeneDx's XomeAnalyzer. Variants identified by WES were evaluated and classified according to published guidelines.[29] The homozygous variant identified in subject 3a was confirmed as homozygous in the similarly affected sibling subject 3b by Sanger sequencing. Whole mitochondrial genome sequencing analysis in blood was performed for subjects 2a and 3a; mtDNA sequence was assembled and analyzed relative to the revised Cambridge Reference Sequence (rCRS) and MITOMAP database as previously described.[29]

Prior to clinical WES, blood DNA from subjects 2a and 2b were also processed for WES in the Mount Sinai Genomics Core Facility using SureSelect V5 libraries (Agilent). Alignment and variant

Table 1. Biochemical and Clinical Characteristics in Individuals with *MRPS34* Variants

Subject Details			*MRPS34* Variants	OXPHOS Enzyme Activities[a]		Clinical Summary		
ID	Sex	Ethnicity	cDNA (GenBank: NM_023936.1); Protein (GenBank: NP_076425.1)	Tissue	Deficient Enzymes	Age of Onset	Clinical Course	Clinical Features and Relevant Family History
S1	male	Italian	c.[321+1G>T]; [321+1G>T], p.[Val100_Gln107del]; [Val100_Gln107del]	muscle liver fibroblasts	CI, CIII, CIV CI, CIV CI, CIV	4 months	died at 9 months	Leigh syndrome,[b] hyperlacticacidemia, microcephaly
S2a	female	Puerto Rican	c.[322−10G>A]; [322−10G>A], p.[Asn108Leufs*12, Asn108Glyfs*50, =]; [Asn108Leufs*12, Asn108Glyfs*50, =]	muscle (19 months) muscle (12 years)	not deficient CI, CIII, CIV	6 months	alive at 17 years	Leigh syndrome,[b] non-verbal, microcephaly, horseshoe kidney, mild coarsening of facial features
S2b	female	Puerto Rican	c.[322−10G>A]; [322−10G>A], p.[Asn108Leufs*12, Asn108Glyfs*50, =]; [Asn108Leufs*12, Asn108Glyfs*50, =]	not performed		6 months	alive at 14 years	Leigh-like syndrome, abnormal MRI, non-verbal, microcephaly, mild coarsening of facial features, sibling of S2a
S3a	female	Puerto Rican	c.[322−10G>A]; [322−10G>A], p.[Asn108Leufs*12, Asn108Glyfs*50, =]; [Asn108Leufs*12, Asn108Glyfs*50, =]	muscle	CI, CII, CIII, CIV	6 months	alive at 7 years	Leigh syndrome,[b] non-verbal, suspected sleep apnea, dysmorphic facies, precocious adrenarche
S3b	female	Puerto Rican	c.[322−10G>A]; [322−10G>A], p.[Asn108Leufs*12, Asn108Glyfs*50, =]; [Asn108Leufs*12, Asn108Glyfs*50, =]	not performed		6 months	alive at 2 years	Leigh syndrome,[b] suspected sleep apnea, sibling of S3a
S4	male	French	c.[37G>A];[94C>T], p.[Glu13Lys];[Gln32*]	muscle fibroblasts	CIV CIV	~10 days	died at 8.5 months	Leigh syndrome,[b] transient metabolic acidosis, hemodynamic instability related to tubulopathy

[a]Activities of OXPHOS enzyme complexes I, II, III, IV (CI, CII, CIII, CIV) were measured in skeletal muscle, liver, or skin fibroblasts; for details see Table S2.
[b]Diagnoses of Leigh syndrome include compatible neuroimaging or postmortem findings.

calling using an in-house GATK-based pipeline, plus variant filtering using Ingenuity Variant Analysis (QIAGEN), were performed as described previously.[30]

WES for subject 4 utilized Agilent SureSelect Human All Exon V libraries. Reads were mapped to the NCBI hg19/GRCh37 human genome reference sequence and variant calling utilized GATK, SAMtools, and Picard Tools. Single-nucleotide variants were called with GATK Unified Genotyper, whereas indel calls were made with the GATK IndelGenotyper_v2. Variants were annotated and filtered using in-house software PolyWeb as described elsewhere.[31]

RNA and DNA Analyses

DNA was extracted from primary skin fibroblasts as described previously.[22] For cDNA studies of subject 1, cultured fibroblasts were grown with and without cycloheximide treatment, as described previously.[32] For cDNA studies of subjects from families 2 and 3, cultured fibroblasts or Epstein-Barr virus-transformed lymphoblasts were grown without cycloheximide treatment. Total RNA was extracted using the miRNeasy Mini kit (QIAGEN) as per manufacturer's protocol and as described previously.[32] Synthesis of cDNA was performed using the SuperScript IV First-Strand Synthesis System (ThermoFisher Scientific) as per manufacturer's protocol and as described previously.[32] To examine the effect of the c.321+1G>T and the c.322−10G>A mutations on mRNA splicing, PCR primers were designed to amplify exons 1–3 of *MRPS34* from cDNA (using either pair 1 [forward primer 5′-CGGGAGCAACT GAACAGG-3′, reverse primer 5′-TGCGTATCCTCTGCACATTC-3′] or pair 2 [forward primer 5′-AGCTCTACGCGGTGGACTAC-3′, reverse primer 5′-GATCCAGGCAGAGAGAGCAC-3′], respectively). PCR products amplified from the *MRPS34* transcript containing the c.322−10G>A mutation were cloned into the pCRTM4-TOPO TA vector using the TOPO TA cloning kit (ThermoFisher Scientific). The vector was transformed into TOP10 competent cells (Invitrogen), and individual colonies were examined and sequenced.

Lentiviral Transduction

For subject 1, lentiviral transduction of fibroblasts was performed as described previously.[22] For subject 4, fibroblasts were transduced with lentiviral particles expressing *RFP* or wild-type *MRPS34* using the p.Lenti7.3 (ThermoFisher Scientific) for 12 hr and then incubated for an additional 20 days until the cells were harvested.

SDS-PAGE and Blue Native Gel Electrophoresis (BN-PAGE)

Protein was extracted from cultured fibroblasts, lymphoblasts, and liver biopsies, and 10–30 μg of each protein lysate was analyzed by SDS-PAGE as described previously.[32,33] BN-PAGE was performed on 100 μg of fibroblast mitochondria lysate in 1% Triton X-100 as described previously[34,35] or on 15 μg fibroblast mitoplast extract in 1% dodecyl maltoside as described previously.[36]

Immunoblotting

Protein lysates analyzed by SDS-PAGE were probed with primary antibodies against MRPS34 (Sigma-Aldrich), MRPL37 (Proteintech or Sigma-Aldrich), MRPL11 (Proteintech), MRPS2 (Abcam), MRPS5 (Abcam), MRPS16 (Proteintech), MRPS18B (Proteintech), MRPS35 (Proteintech), GAPDH (Cell Signaling), NDUFS3 (Abcam), complex II 70 kDa subunit (Molecular Probes), COXI (Abcam), VDAC1 (MitoSciences or Abcam), Beta-Actin (Abcam), Citrate Synthase (GeneTex), and Total OXPHOS Human WB Antibody Cocktail (consisting of five antibodies: ATP5A, UQCRC2, SDHB, COXII, and NDUFB8; Abcam). Isolated mitochondria and mitoplasts analyzed by BN-PAGE were probed with Total OXPHOS Rodent WB Antibody Cocktail (consisting of five antibodies: ATP5A, UQCRC2, COXI, SDHB, and NDUFB8; Abcam) or with primary antibodies against NDUFA13, SDHA, UQCRC2, COXIV, and ATP5A (Abcam), respectively. Blots were incubated with anti-mouse or anti-rabbit IgG secondary antibodies (VWR International) and developed with Clarity Western ECL Substrate (Bio-Rad Laboratories) or with IRDye 800CW/680LT Goat Anti-Rabbit or Anti-Mouse IgG (Li- Cor) secondary antibodies and visualized using an Odyssey Infrared Imaging System (Li-Cor). Relative band intensities were quantitated using ImageJ software, where protein levels were normalized to VDAC1.

Sucrose Gradient Subfractionation

Fibroblast mitochondria were prepared from 8 × 15 cm^2 dishes as described previously,[37] and the isolated mitochondria were lysed with 2% digitonin in 260 mM sucrose, 10 mM Tris HCl (pH 7.5), 100 mM KCl, and 20 mM $MgCl_2$ in the presence of 1× Complete EDTA-free Protease inhibitor cocktail for 20 min as previously described.[38] The mitochondrial lysate was centrifuged for 45 min at 9,200 × *g* at 4°C and the clarified lysate was loaded onto a continuous 10%–30% sucrose gradient (in 10 mM Tris-HCl [pH 7.4], 100 mM KCl, 20 mM $MgCl_2$ in the presence of protease inhibitors) and centrifuged at 71,000 × *g* in an Optima Beckman Coulter preparative ultracentrifuge for 15 hr. Fractions were collected and precipitated with 0.02% sodium deoxycholate and 12% trichloroacetic acid (final concentration) and washed twice with acetone, and the entire precipitate was resolved by SDS-PAGE. Protein markers of the mitochondrial ribosomal subunits were detected by immunoblotting, as described above.

Mitochondrial Protein Synthesis Assay

Mitochondrial protein synthesis was analyzed in fibroblasts using previously described methods.[37,39–41]

Quantitative Proteomics

Mass spectrometry on primary fibroblast material was performed label-free, using sample preparation methodology previously described with modifications.[42] Fibroblasts from three separate control subjects and two subcultures of subject 1 cultured as above were solubilized in 1% w/v sodium deoxycholate, 100 mM Tris-HCl (pH 8.1) prior to incubation at 99°C for 10 min with vortexing. Samples were further incubated for 10 min at 60°C in a sonicator waterbath, followed by the addition of 5 mM Tris(2-carboxyethy)phosphine (TCEP), 20 mM chloroacetamide and incubation for 5 min at 99°C with vortexing. Denatured and alkylated proteins were digested with trypsin overnight at 37°C. Detergent was removed by extraction into ethyl acetate in the presence of 2% formic acid (FA), followed by concentration of the aqueous phase through vacuum centrifugation. Peptides reconstituted in 0.5% FA were loaded onto small cation exchange (Empore Cation Exchange-SR, Supelco Analytical) stage-tips made in-house.[43] Tips were washed with 20% acetonitrile (ACN), 0.5% FA and eluted over five fractions of increasing amounts (45−300 mM) freshly prepared ammonium acetate, 20% ACN, 0.5% FA, followed by a final elution of 5% ammonium hydroxide, 80% ACN. Fractions were concentrated by vacuum centrifugation and desalted on SDB-XC poly(styrene-divinyl-benzene; Supelco Analytical) stage-tips as previously described.[40,43] Peptides were reconstituted in 0.1% trifluoroacetic acid (TFA) and 2% ACN and analyzed by online nano-HPLC/electrospray ionization-MS/MS on a Q Exactive Plus connected to an Ultimate 3000 HPLC (Thermo-Fisher Scientific). Peptides were loaded onto a trap column (Acclaim C_{18} PepMap nano Trap × 2 cm, 100 μm I.D, 5 μm particle size, and 300 Å pore size; ThermoFisher Scientific) at 15 μL/min for 3 min before switching the pre-column in line with the analytical column (Acclaim RSLC C_{18} PepMap Acclaim RSLC nanocolumn 75 μm × 50 cm, PepMap100 C_{18}, 3 μm particle size 100 Å pore size; ThermoFisher Scientific). The separation of peptides was performed at 250 nL/min using a non-linear ACN gradient of buffer A (0.1% FA, 2% ACN) and buffer B (0.1% FA, 80% ACN), starting at 2.5% buffer B to 35.4% followed by ramp to 99% over 120 min. Data were collected in positive mode using Data Dependent Acquisition using m/z 375–1,800 as MS scan range, HCD for MS/MS of the 12 most intense ions with $z \geq 2$. Other instrument parameters were: MS1 scan at 70,000 resolution (at 200 m/z), MS maximum injection time 50 ms, AGC target 3E6, Normalized collision energy was at 27% energy, Isolation window of 1.8 Da, MS/MS resolution 17,500, MS/MS AGC target of 1E5, MS/MS maximum injection time 100 ms, minimum intensity was set at 1E3, and dynamic exclusion was set to 15 s.

Raw files were analyzed using the MaxQuant platform[44] v.1.5.5.1 searching against the Uniprot human database containing reviewed, canonical, and isoform variants in FASTA format (June 2016) and a database containing common contaminants. Default search parameters for a label-free (LFQ) experiment were used. Briefly, multiplicity was set to 1 (unlabeled), "LFQ," "Requantify," and "Match between runs" were enabled with default settings. Unique and razor peptides were used for quantification, using a minimum ratio count of 2. Using the Perseus platform v.1.5.5.3,[45] proteins identified using <2 unique peptides were excluded, as were identifications marked "Only identified by site," "Reverse," and "Potential contaminant." Mitochondrial proteins were defined through matching of gene names and Ensembl gene IDs to the Mitocarta2.0 dataset.[46] LFQ Intensity values were Log_2 transformed, and mean and standard deviations were calculated for each experimental group, consisting of either three control fibroblast biological replicates or two subject fibroblast technical replicates. Values from a group with a standard deviation > 0.3 were invalidated by conversion to "NaN" and rows were filtered to contain at least two valid values in both experimental groups. A two-tailed ratio paired t test was performed on the linearized Log2 LFQ Intensity Mean values for controls and

subject 1. The D'Agostino and Pearson normality test was used to confirm that the log of the ratios followed a Gaussian distribution. The Bonferroni correction was used to determine the p value threshold for significance.

Mapping of subunit levels to complex I (PDB: 5LDW) was performed as previously described.[42,47] For mitoribosome subunit mapping, the human mitoribosome structure (PDB: 3J9M) was used.[48] For complexes III and IV, homologous human subunits were mapped to the bovine structures PDB: 1BGY and 5B1A, respectively,[49,50] whereas for complex II homologous human subunits were mapped to those found in the porcine structure (PDB: 1ZOY).[51]

Results

Whole-Exome Sequencing Identified *MRPS34* Autosomal-Recessive Mutations in Individuals with Leigh(-like) Syndrome

We analyzed six subjects from four families with Leigh or Leigh-like syndrome and OXPHOS defects (Figure 1A and Table 1). WES studies identified homozygous or compound heterozygous pathogenic variants in *MRPS34* (GenBank: NM_023936.1) in all subjects, which were confirmed by Sanger sequencing (Figure 1B). A homozygous essential splice site mutation, c.321+1G>T, was identified in subject 1, an Australian child with consanguineous parents of Italian ancestry. This variant is predicted to cause abnormal splicing by abolishing the donor splice site of exon 1. The *MRPS34* c.321+1G>T variant is absent from dbSNP and the Genome Aggregation Database (gnomAD) Browser.[52,53] A homozygous extended splice site mutation, c.322−10G>A, was identified in subjects 2a, 2b, 3a, and 3b of Puerto Rican ethnicity; these subjects were ascertained with assistance from the GeneMatcher tool.[54] This variant is predicted to abolish the acceptor splice site and create a new cryptic splice acceptor site within intron 1, causing abnormal gene splicing. The *MRPS34* c.322−10G>A variant is reported in dbSNP (rs563189672), and two heterozygous individuals (both of Latino ethnicity) were reported in the gnomAD Browser (2 of 236,804 alleles examined, no homozygotes observed). Principal component analysis of available WES data revealed that individuals from families 2 and 3 all fall in the admixed American (AMR) group, and their close clustering indicated that they come from a very similar population (Table S3 and Figure S2). Kinship analysis showed that there is no consanguinity at the level of second cousins or closer between the parents either within or across families 2 and 3 (Table S4). Analysis of the variants in the *MRPS34* genomic region using WES data from families 2 and 3 showed a shared haplotype of ~590 kb in size between chr16: 1,306,986–1,894,912 (Table S5), implying that the c.322−10G>A mutation is a founder mutation.

Compound heterozygous *MRPS34* mutations were identified in subject 4: a c.37G>A (p.Glu13Lys) missense variant and a c.94C>T (p.Gln32*) nonsense variant. The c.37G>A (p.Glu13Lys) variant is absent from dbSNP and the gnomAD Browser. Protein sequence alignment of human MRPS34 with its homologs in nine other vertebrate species indicated that the p.Glu13 residue is highly conserved (Figure 1C). The *MRPS34* c.37G>A (p.Glu13Lys) missense variant is predicted as damaging by SIFT (score 0.02), disease causing by MutationTaster (score 1.0), probably damaging by PolyPhen-2 (score 0.97), and likely to interfere with function by AlignGVD (class C55, second highest class of 7). The *MRPS34* c.94C>T (p.Gln32*) variant is reported in dbSNP (rs763672163), and 39 heterozygous individuals were reported in the gnomAD Browser (39 of 82,878 alleles examined, no homozygotes observed). Investigation of family members with DNA available confirmed that all variants segregated with disease (Figures 1A and 1B). The *MRPS34* variants not reported in dbSNP have been submitted to ClinVar (see Accession Numbers).

The *MRPS34* c.321+1G>T and c.322−10G>A Mutations Cause Abnormal mRNA Splicing

The c.321+1G>T variant (subject 1) lies within the highly conserved donor splice site of exon 1, while the c.322−10G>A variant (families 2 and 3) is situated within the extended acceptor site of exon 2. To examine the effect of these variants on *MRPS34* splicing, PCR was performed on cDNA synthesized from fibroblast or lymphoblast RNA extracted from control individuals and subjects 1 and 2a. For the c.321+1G>T variant, gel electrophoresis of PCR products containing exons 1–3 of *MRPS34* revealed an amplicon in subject 1 that was smaller than that in control (Figure 2A). Sequencing determined that this amplicon lacked the last 24 bases of exon 1, indicating the use of an upstream donor splice site within exon 1 (Figure 2B). The c.321+1G>T variant therefore produces a shortened, stable transcript that results in an in-frame deletion of eight amino acids, p.Val100_Gln107del (Figure 2C). Protein sequence alignment of human MRPS34 with its homologs in nine other vertebrate species indicated that the missing eight amino acids are highly conserved (Figure 2D).

To determine the effect of the c.322−10G>A variant on splicing, *MRPS34* PCR products amplified from fibroblast and lymphoblast cDNA were cloned and sequenced. Two abnormally spliced *MRPS34* transcripts resulting in frameshifts and premature truncations were detected in subject 2a; an amplicon with eight nucleotides inserted prior to exon 2 due to the utilization of a cryptic intronic acceptor site (p.Asn108Leufs*12), which represented 80% or 68% of total PCR products analyzed in fibroblasts and lymphoblasts, respectively, and an amplicon which skipped exon 2 (p.Asn108Glyfs*50) observed in 10% or 18% of total PCR products analyzed in fibroblasts or lymphoblasts, respectively. The remaining analyzed PCR products were wild-type (10% or 15% in fibroblasts and lymphoblasts, respectively) (Figure 2C). Quantitative RT-PCR analysis of fibroblast cDNA revealed a ~75% reduction in *MRPS34* transcript level in cells from subject 3a relative to control (Figure S3). Collectively, these results confirm that the

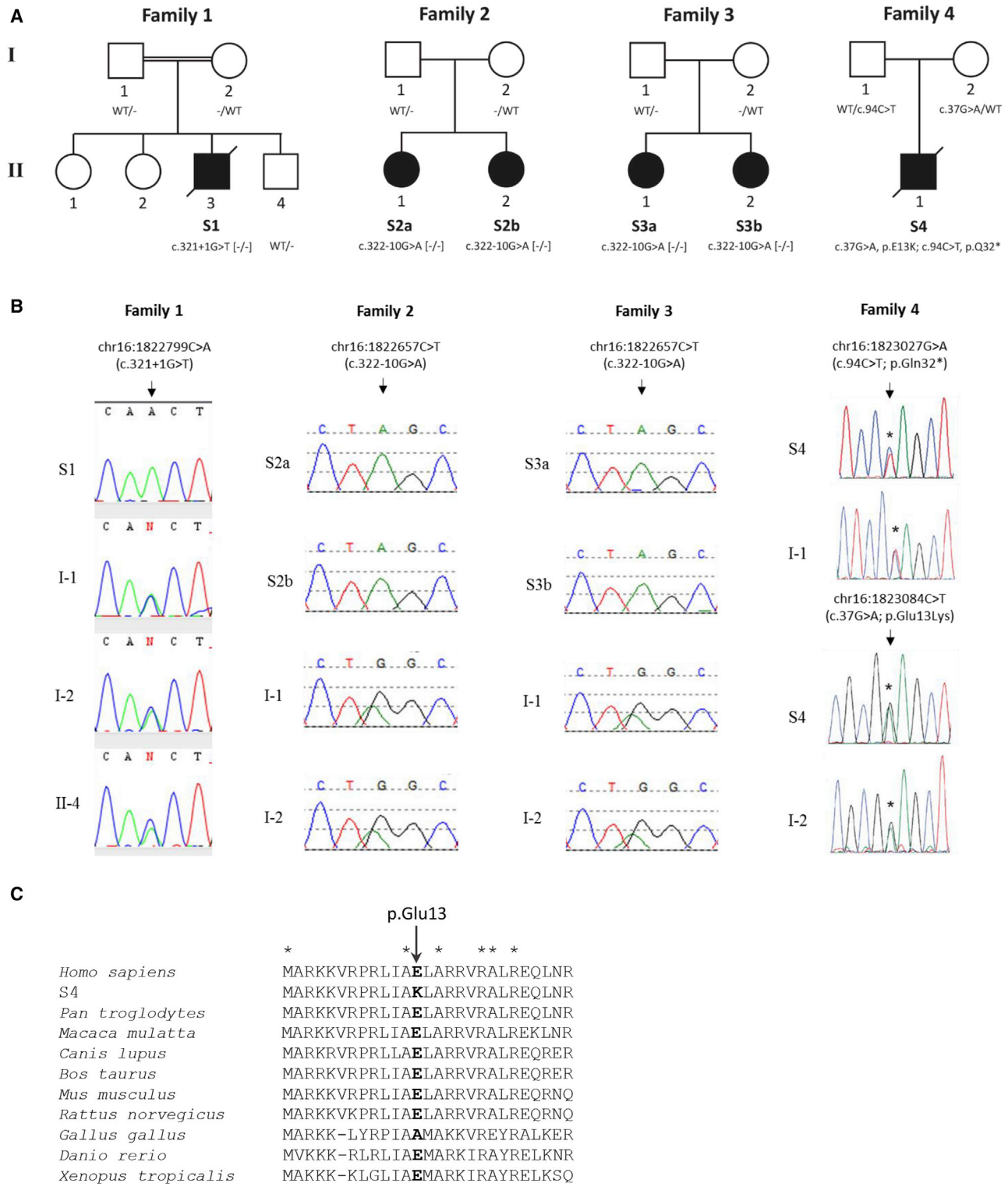

Figure 1. Identification of *MRPS34* Mutations in Six Subjects from Four Families
(A) Pedigrees and genotype of subjects with *MRPS34* variants. Minus sign (−) denotes a mutant allele.
(B) Sequencing chromatograms confirming the *MRPS34* variants in affected subjects and the carrier status of family members with DNA available.
(C) Protein sequence alignment of human MRPS34 with its homologs in nine other vertebrate species showing the conservation of the p.Glu13 residue mutated in family 4. Asterisks (*) depict conserved amino acids.

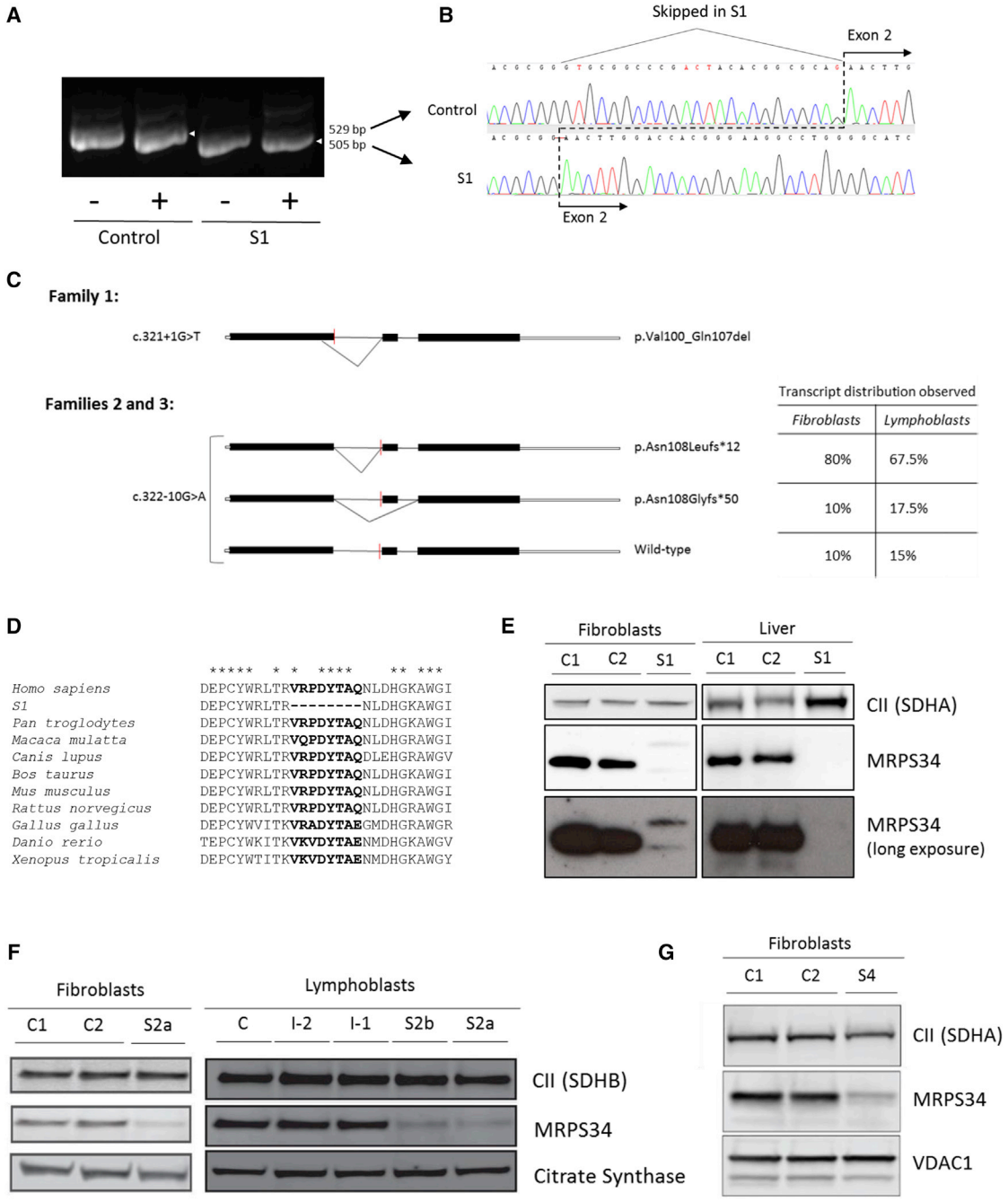

Figure 2. Characterization of MRPS34 in Affected Subjects with *MRPS34* Mutations

(A) PCR amplicons of *MRPS34* exons 1–3 generated from control individual and subject 1 fibroblast cDNA ± cycloheximide (CHX). The amplicon detected in subject 1 was smaller than the control amplicon.

(B) Sequence analysis of the *MRPS34* cDNA PCR amplicon detected in subject 1 identified a 24 bp deletion corresponding to the utilization of an upstream donor site in exon 1. This splicing mutation therefore produces a shortened transcript that results in an in-frame deletion of eight amino acids, p.Val100_Gln107del.

(C) Schematic diagram depicting the abnormal transcript generated from the c.312+1G>T variant (family 1) and two abnormal plus residual wild-type transcript generated from the c.322−10G>A variant (families 2 and 3). The distribution of the three transcripts generated from the c.322−10G>A variant in S2a fibroblasts (40 clones sequenced) and lymphoblasts (40 clones sequenced) is additionally described in the table. The red line indicates the position of the variant. The diagram solid black bars represent exons, while the open bars represent untranslated region.

(D) Protein sequence alignment of human MRPS34 with its homologs in nine other vertebrate species. Asterisks (*) depict conserved amino acids. The eight amino acids missing from the MRPS34 protein produced in subject 1 are highly conserved across the species examined.

(legend continued on next page)

c.321+1G>T and c.322−10G>A variants cause impaired splicing of the *MRPS34* transcript. The latter variant allows some wild-type mRNA to be made, implying that it is a hypomorphic allele.

MRPS34 Protein Levels Are Reduced in Individuals with *MRPS34* Recessive Mutations

To investigate the effect of the mutations on MRPS34 protein levels, immunoblotting was performed on available tissue and cells from control individuals and subjects 1, 2a, 2b, and 4. Immunoblotting of fibroblasts and liver tissue confirmed the absence of wild-type MRPS34 protein in subject 1 (Figure 2E), and longer exposure of the immunoblots revealed two bands in subject 1 that were faint but detectable, one of which may represent the mutant MRPS34 protein (p.Val100_Gln107del). These results suggest that the mutant MRPS34 protein is likely degraded in subject 1. In cells from subjects 2a, 2b, and 4, a substantial decrease in MRPS34 protein levels was identified relative to controls (Figures 2F and 2G). The residual protein in subjects 2a and 2b with the homozygous c.322−10G>A mutation likely reflects the presence of residual wild-type transcript. These findings establish that all the *MRPS34* mutations identified in the affected subjects result in decreased MRPS34 protein levels.

Individuals with *MRPS34* Mutations Have Combined OXPHOS Deficiency Associated with Reduced Mitochondrial Translation

Spectrophotometric enzyme assays performed on liver, skeletal muscle, and/or fibroblasts identified a combined OXPHOS deficiency in subjects 1, 2a, and 3a, and isolated complex IV deficiency in subject 4 (Table S2). Immunoblotting of cell lysates from control individuals and subjects 1, 2a, 2b, and 4 revealed decreased levels of OXPHOS complex I and IV subunits in affected subjects relative to control subjects (Figures 3A–3C). This was associated with a decrease in the steady-state levels of assembled complexes I and IV in fibroblasts from subject 1, as demonstrated by BN-PAGE (Figure 3D). BN-PAGE also showed a decrease in assembled complex I in subject 4, but complex IV assembly was not clearly decreased below controls (Figure 3E). Given that MRPS34 is a component of the mitoribosome, we sought to determine whether the combined OXPHOS deficiency was due to reduced mitochondrial translation. Examination of mitochondrial de novo protein synthesis in fibroblasts from subjects 1 and 4 by ^{35}S-methionine radiolabeling revealed an overall decrease in protein synthesis of mtDNA-encoded OXPHOS subunits in the affected subjects relative to control individuals (Figures 3F, 3G, and S4). BN-PAGE analysis of pulse-chase ^{35}S-methionine labeled mitochondrial lysates suggested that subject 1 cells had a reduced rate of complex IV formation relative to control (Figure 3H). These findings demonstrate that MRPS34 is required for efficient mitochondrial translation in humans.

MRPS34 Mutation Reduces Mitochondrial Translation by Destabilizing the Small Mitoribosomal Subunit

We have previously established that decreased protein levels of MRPS34 in mice with a *Mrps34* missense mutation destabilized the small mitoribosomal subunit.[18] To determine the effect of *MRPS34* mutation on the stability of the small mitoribosomal subunit in affected human subjects, we investigated the steady-state levels of other small mitoribosomal subunit proteins in fibroblast lysates from control individuals and subjects 1 and 4 by immunoblotting. The steady-state abundance of various small mitoribosomal subunit proteins was reduced in subjects 1 and 4 relative to control individuals (Figures 4A and 4B). Interestingly, the abundance of large mitoribosomal subunit proteins was not affected by the *MRPS34* mutation (Figures 4A and 4B). To investigate how the decrease in small mitoribosomal subunit proteins affects the mitoribosome, we analyzed the profile of the large and small mitoribosomal subunits, as well as the monosome and polysome, in fibroblast mitochondrial lysates using sucrose gradients. Immunoblotting of the sucrose gradient fractions showed a decrease in actively translating mitochondrial ribosomes in subject 1 relative to a control individual (Figure 4C). In mitochondria isolated from subject 1 cells, the mitoribosomal proteins of the small and large subunits are both redistributed toward the top of the gradient compared to those in mitochondria from control cells, indicating that a subunit assembly defect occurred in subject 1 (Figure 4C). Reduced levels of the monosome in the cells from subject 1 further indicates that the mitoribosome is destabilized by having reduced MRPS34 protein levels, which precludes correct assembly of the small ribosomal subunit and consequent association with the large subunit. Overall, these results are consistent with those observed in the *Mrps34* mutant mouse[18] and confirm that mutation of *MRPS34* destabilizes the small ribosomal subunit, resulting in impaired mitochondrial translation.

Quantitative proteomic analysis of fibroblasts from subject 1 relative to three independent control samples was also performed to permit unbiased detection of global cellular protein changes that result from the *MRPS34* mutation (Table S6). Approximately 4,500 total proteins were quantified across all samples by this approach, of which

(E) SDS-PAGE western blot of MRPS34 and complex II 70 kDa subunit SDHA (loading control) from control individuals (C1 and C2) and subject 1 fibroblasts and liver showed the absence of wild-type MRPS34 protein in subject 1. Long exposures revealed faint double banding in subject 1 fibroblast samples probed with MRPS34 antibody.
(F and G) SDS-PAGE western blot of MRPS34 in fibroblasts and lymphoblasts revealed a substantial decrease in MRPS34 levels in subjects 2a (F), 2b (F), and 4 (G) relative to control individuals (C1 and C2) and to parental samples (I-2 and I-1 from family 2). Complex II subunits SDHA and SDHB, VDAC1, and citrate synthase represent loading controls.

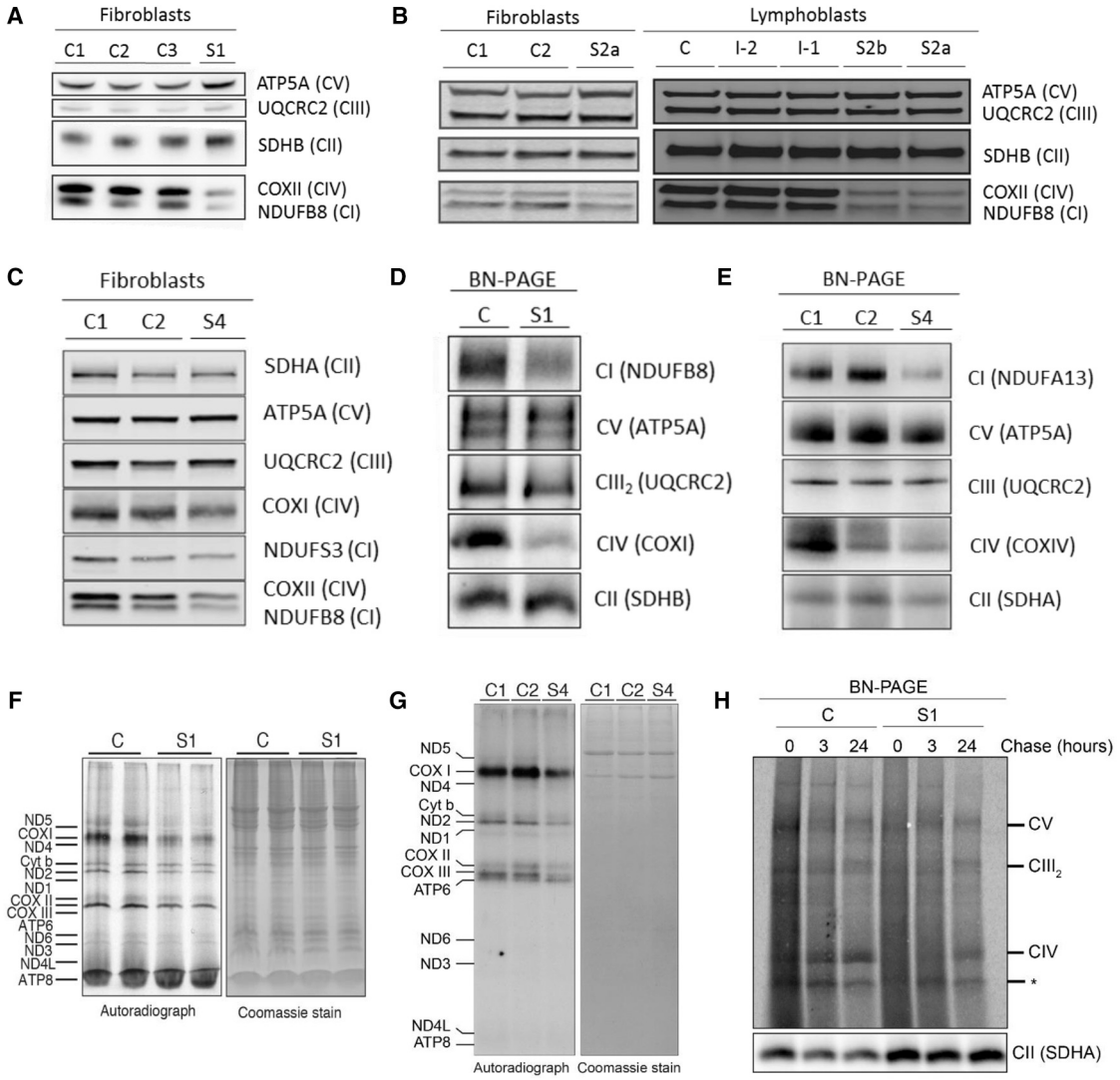

Figure 3. Evidence of Combined OXPHOS Deficiency and Reduced Mitochondrial Translation in Affected Subjects with *MRPS34* Mutations

(A–C) SDS-PAGE western blot of protein from fibroblasts and lymphoblasts showed reduced levels of complex I (CI) and complex IV (CIV) subunits in subjects 1 (A), 2a (B), 2b (B), and 4 (C) relative to control individuals (C1–C3) and to parental samples (I-2 and I-1 from family 2). Complex II subunits (SDHA and SDHB) are indicative of loading.

(D and E) BN-PAGE western blot of fibroblast protein showed reduced levels of CI and CIV in subjects 1 (D) and 4 (E) relative to control individuals (C, C1, and C2). Complex II (SDHA and SDHB) is indicative of loading.

(F and G) Protein synthesis in cell lysates was measured by pulse incorporation of ^{35}S-labeled methionine and cysteine. Equal amounts of cellular protein were separated by SDS-PAGE and visualized by autoradiography. The in vitro pulse labeling of mitochondrial translation products revealed decreased levels of mtDNA-encoded subunits in subject 1 (F) and subject 4 (G) relative to control individuals (C1 and C2). The Coomassie stain represents relative loading.

(H) Examination of mitochondrial protein synthesis in control individual (C) and subject 1 fibroblasts by [^{35}S]-methionine radiolabelling. Isolated mitochondria were subject to BN-PAGE, following which the complexes were visualized by autoradiography. A slower formation of complex IV was observed in subject 1 relative to control individual. SDHA was used as a loading control. Asterisk (*) denotes a non-specific band.

753 were mitochondrial proteins, including 27 proteins of the small mitoribosome subunit and 47 large subunit proteins. The abundance of all detected small mitoribosome subunit proteins was significantly decreased in the subject's cell line compared to control individuals, while none of the proteins from the large mitoribosome subunit were substantially altered (Figures 5A and 5B). Figure 5C and Movie S1 show the changes in protein abundance between subject 1 and control individuals mapped to the human mitoribosome structure, as we have done previously for complex I.[42] These representations clearly illustrate the marked decrease in small mitoribosomal subunit proteins in subject 1 compared to control individuals, as well as the relative sparing of the large subunit, consistent with destabilization of the small mitoribosomal subunit. Mapping of protein levels to the structures of OXPHOS

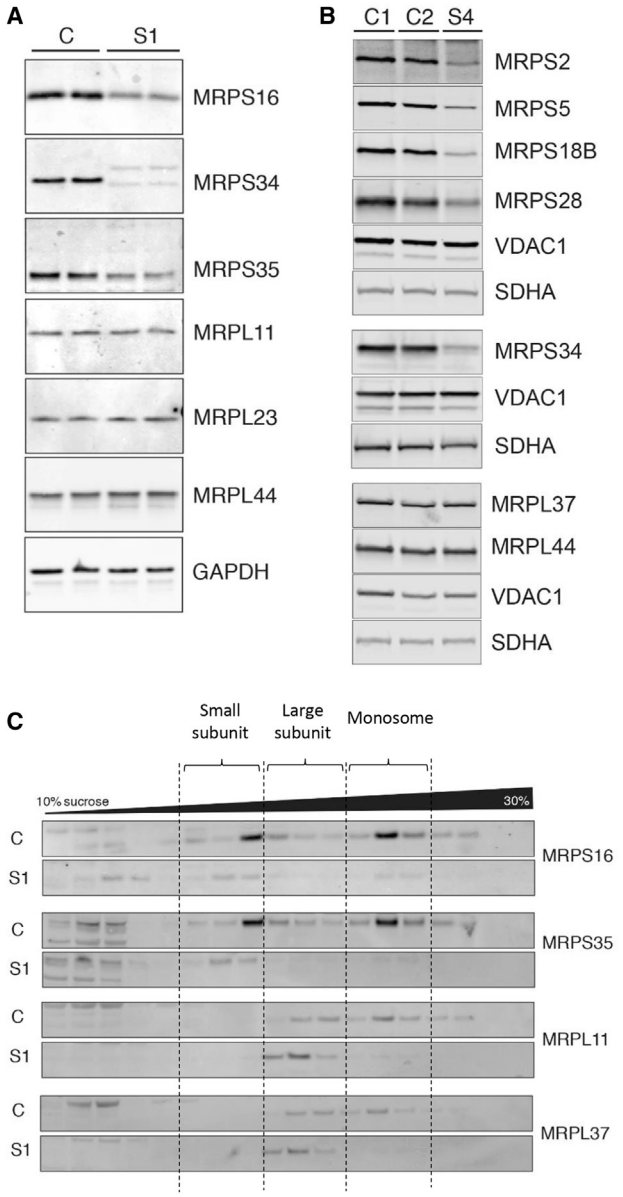

Figure 4. MRPS34 Mutations Are Associated with Reduced Protein Levels of Small Mitoribosomal Subunits and Destabilization of the Mitoribosome

(A and B) SDS-PAGE western blot of protein from fibroblasts showed reduced protein levels of small mitoribosomal subunit proteins in subjects 1 (A) and 4 (B) relative to control individuals (C1 and C2). The abundance of large mitoribosomal proteins in subjects 1 and 4 were comparable to control individuals. Complex II subunit SDHA, VDAC1, and GAPDH were used as loading controls.

(C) A continuous 10%–30% sucrose gradient was used to determine the distribution of the small and large ribosomal subunit and the monosome in mitochondria isolated from control individual (C) and subject 1 cells. Mitochondrial ribosomal protein markers of the small (MRPS16 and MRPS35) and large (MRPL11 and MRPL37) ribosomal subunits were detected by immunoblotting with specific antibodies. The data are representative of results from three independent biological experiments. The dashed vertical lines denote the relevant fractions as indicated.

complexes I–IV showed general turnover of the subunits of complexes I and IV, and to a lesser extent complex III (Figure 5D), with a trend to increase seen for complex II, consistent with reduced translation of mtDNA-encoded mRNAs. As a group, complex I and complex IV protein subunits were significantly decreased in subject 1 relative to control individuals (Figure 5B and Table S7). Interestingly, the mean subunit level of each OXPHOS complex closely matched the residual enzyme activity in the subject's fibroblasts (Tables S2 and S7). The quantitative proteomic data therefore validate destabilization of the small mitoribosomal subunit and the consequent impact on mitochondrial translation in subject 1.

Lentiviral-Mediated Expression of Wild-Type *MRPS34* in Fibroblast Cells from Two Affected Subjects Rescues Dysfunctional Mitochondrial Translation and OXPHOS Capacity

To validate the pathogenicity of *MRPS34* mutations, we performed complementation studies to determine whether expression of wild-type *MRPS34* in subject cells rescued the mitochondrial translation defect. Fibroblasts from control, subject 1, and a subject with a homozygous pathogenic mutation in *MRPS7*[8] were transduced with a lentiviral vector expressing wild-type *MRPS34*. The levels of complex IV mtDNA-encoded subunit COXII and complex I nuclear-encoded subunit NDUFB8, a marker of complex I stability, were examined by immunoblotting. Densitometry analysis confirmed a decrease in COXII and NDUFB8 protein levels in subject 1 and in the subject with *MRPS7* mutations relative to control (Figures 6A–6C). Lentiviral-mediated expression of wild-type *MRPS34* caused a significant increase in COXII and NDUFB8 in subject 1, but not in the cell line from the subject with *MRPS7* mutations (Figures 6A–6C), confirming that the disorder of mitochondrial translation in subject 1 is due specifically to loss-of-function mutations in *MRPS34*. Measurement of complex I and complex IV activities using enzyme dipstick assays confirmed that lentiviral-mediated expression of wild-type *MRPS34* significantly increased complex I and complex IV activity in cells from subject 1, but not in cells from the subject with *MRPS7* mutations (Figures 6D and 6E). Lentiviral-mediated expression of *MRPS34* in control cells caused a modest decrease in complex IV activity, suggesting a potential negative effect of *MRPS34* overexpression in cells with a stable small mitoribosomal subunit, though not in contradiction with the rescue observed in cells from subject 1. To further support *MRPS34* mutation pathogenicity, cells from subject 4 with compound heterozygous *MRPS34* mutations that had been transduced with lentiviral particles expressing wild-type *MRPS34* showed increased levels of small mitoribosomal subunit proteins MRPS5 and MRPS18B relative to cells transduced with red fluorescent protein (Figure 6F). These results provide further evidence that wild-type *MRPS34* rescue stabilized the small mitoribosomal subunit. Collectively, these data

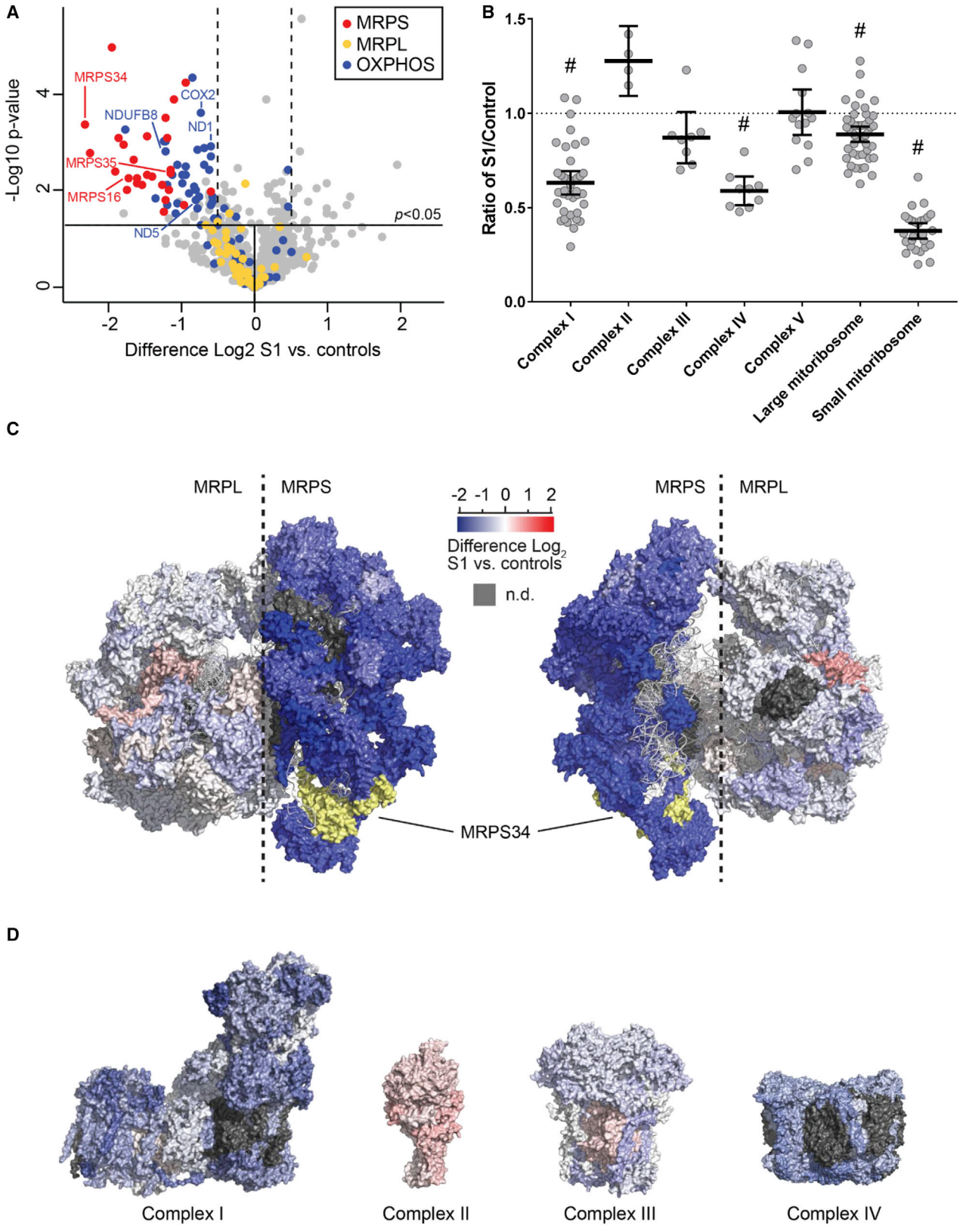

Figure 5. Quantitative Proteomic Analysis of Fibroblasts from an Affected Subject with *MRPS34* Mutations Identifies a General Decrease in Small Mitoribosomal and OXPHOS Subunit Proteins

(A) Quantitative mass spectrometry of mitochondrial proteins in fibroblasts from subject 1 and control individuals demonstrates down-regulation of small mitoribosome subunits (red dots), as well as OXPHOS subunits (blue dots), in subject 1. In contrast, the levels of large mitoribosome subunits (yellow dots) in subject 1 are generally unaffected. Proteins examined in this study by SDS-PAGE and observed to have reduced levels are indicated by the text labels. The horizontal line within the volcano plot represents a significance value of

(legend continued on next page)

establish that recessive mutations in *MRPS34* cause Leigh syndrome.

Discussion

We describe six patients from four unrelated families in whom autosomal-recessive missense, nonsense, or splice site mutations in *MRPS34* caused instability of the small mitoribosomal subunit, impaired mitochondrial translation, and defective OXPHOS capacity. Subjects with *MRPS34* mutations developed Leigh or Leigh-like syndrome, involving metabolic strokes associated with early developmental delay and/or regression. Additional clinical features including microcephaly and dysmorphic facies were also observed in several subjects. Our study expands the known genetic causes of Leigh(-like) syndrome to now include mutations in a gene that encodes a small mitoribosomal protein.[19] While Leigh-like lesions were observed in an adult subject with mutations in *MRPL44* and a clinical presentation characterized by hypertrophic cardiomyopathy, hemiplegic migraine, and exercise-induced muscle pain,[16] our study broadens the clinical heterogeneity of human disorders of the mitoribosome to also include infantile-onset Leigh(-like) syndrome. To date, pathogenic mutations in ~10% of all genes encoding mitoribosomal proteins have been described to cause disease. This observation is particularly striking in the context that mutations in nearly all of the genes encoding mitochondrial aminoacyl-tRNA synthetases, which are also required for mitochondrial translation, have been described to cause clinical disease.[55,56] This contrast, alongside data indicating that a similar proportion of proteins within each group were required for OXPHOS in cell models,[17] suggests an intriguing discrepancy between these two gene groups in how pathogenic mutations have been accumulated and tolerated at a population level.

Although all affected subjects experienced disease onset in early infancy, there was variability in disease severity across the cohort. Early death of subjects 1 and 4 occurred within the first year of life, while survival into childhood and late adolescence is seen in subjects from families 2 and 3. The longer survival in these subjects with the homozygous *MRPS34* c.322−10G>A variant could be related to this mutation acting as a hypomorphic allele, as we showed that small amounts of wild-type transcript are generated in these subjects' fibroblasts and lymphoblasts. To our knowledge, the *MRPS34* c.322−10G>A variant has been identified only in individuals of Latino ethnicity, including the eight individuals from families 2 and 3 of Puerto Rican descent and the two heterozygous Latino individuals reported in gnomAD, suggesting that this variant may represent a founder mutation. Analysis of the available WES data from families 2 and 3 revealed that the *MRPS34* c.322−10G>A variant lies within a shared haplotype, providing further evidence of a founder effect. The *MRPS34* c.322−10G>A variant should therefore be considered in subjects of Puerto Rican descent with Leigh(-like) syndrome and OXPHOS defects.

Demonstration of impairments in OXPHOS enzyme activities, mitochondrial translation activity, and mitoribosome assembly in affected subjects provided several lines of evidence to support the pathogenicity of biallelic *MRPS34* mutations. The rescue of cellular defects associated with impaired mitochondrial translation by lentiviral-mediated expression of wild-type *MRPS34* transcript in fibroblasts from affected subjects further establishes that recessive pathogenic mutations in *MRPS34* cause disease. Quantitative proteomics further confirmed the cellular effects of *MRPS34* mutation, identifying a general decrease in the level of proteins from the small mitoribosomal subunit and OXPHOS complexes I and IV, which were strikingly consistent with enzyme activity results. We recently demonstrated the utility of this profiling technique for identifying proteomic signatures of expression changes in response to knockout of individual subunits of OXPHOS complex I in gene-edited cell lines relative to isogenic controls.[42] Here, we further demonstrate that it can also serve as an effective tool for detecting specific proteomic signatures in fibroblasts from subjects relative to fibroblast controls from varied genetic backgrounds. Indeed, in the absence of any prior knowledge of disease causation, quantitative proteomic analysis of fibroblasts from subject 1 would have identified MRPS34 as the most reduced mitochondrial protein. The decreased amounts of all other small ribosomal subunit proteins and subunits from OXPHOS complexes I and IV provide further direct support for a defect in stability of the small mitoribosome subunit. Quantitative proteomics therefore represents a powerful approach to elucidate the pathogenicity of novel gene mutations, with broad utility likely beyond investigation of primary mitochondrial disorders.

The mitoribosomal subunit assembly process in humans is poorly understood.[2] Our data from cells of a subject with

$p = 0.05$, where the levels of proteins represented above the horizontal $p = 0.05$ line was regarded as significantly different from control individuals. The two dashed vertical lines indicate Log2 changes of >0.5 up- or downregulation relative to control individuals.
(B) OXPHOS and mitoribosome protein levels in subject 1 represented as a ratio of the control mean. Hashes denote groups that were significantly reduced in subject 1 relative to control individuals (all with p value < 0.0001). The middle bar represents the mean value, while the upper and lower bars represent the 95% confidence interval of the mean value. Each dot represents a single protein.
(C) Changes in mitoribosome protein levels between subject 1 relative to control individuals mapped to the structure of the human mitoribosome. As per the inset scale, proteins colored in blue are decreased, and those colored in red are increased, in subject 1 relative to control individuals. Grey indicates no data; yellow indicates MRPS34.
(D) Changes in OXPHOS subunit levels for complexes I–IV mapped to homologous subunits of the relevant structure. Color scale as per (C).

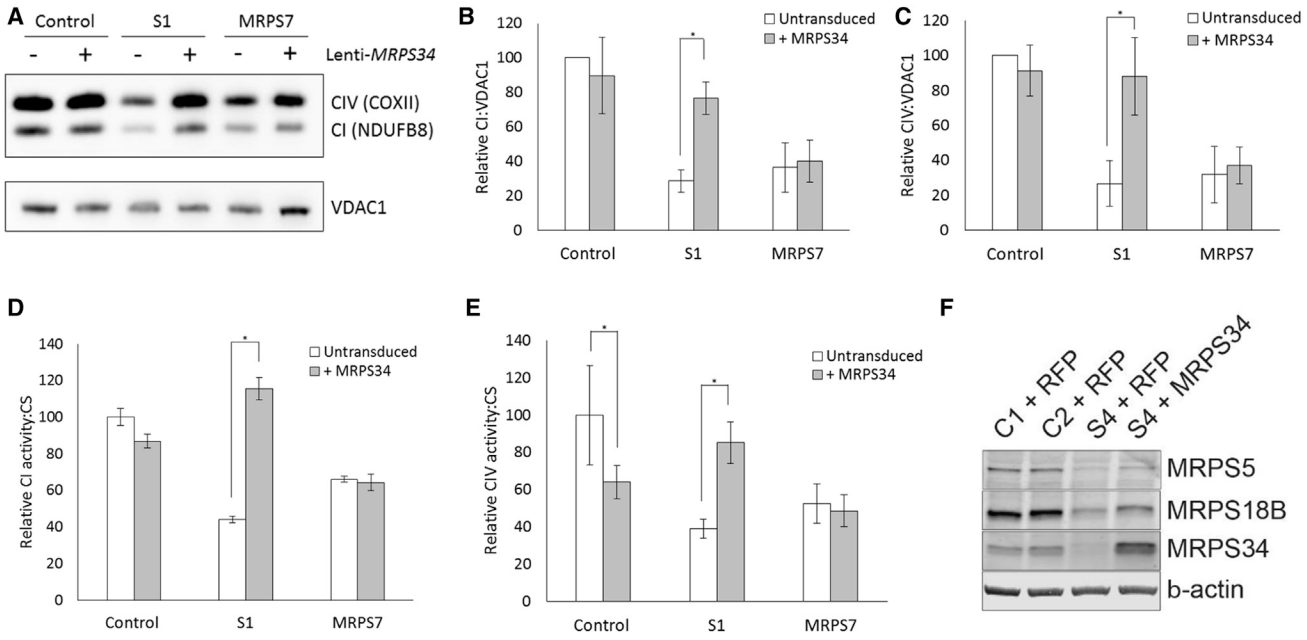

Figure 6. Lentiviral-Mediated Expression of Wild-Type *MRPS34* Rescues the Defect in Mitochondrial Translation in Cells from Affected Subjects

(A) Fibroblasts from control individual, subject 1, and a subject with pathogenic *MRPS7* variants were transduced with wild-type *MRPS34* cDNA. Representative SDS-PAGE western blot demonstrates an increase in protein levels of CI (NDUFB8) and CIV (COXII) subunits in subject 1 fibroblasts transduced with *MRPS34* relative to untransduced cells. VDAC1 was used as a loading control.

(B and C) Densitometry analysis revealed that the increase in CI subunit NDUFB8 (B) and CIV subunit COXII (C) observed in subject 1 fibroblasts transduced with *MRPS34* relative to untransduced cells was significant ($p = 0.0049$ and 0.036, respectively). Results were normalized to VDAC1 and presented as the percent of average untransduced control cells. The data represent the mean of three independent transfections ± SEM.

(D and E) Complex I (D) and complex IV (E) activity was measured in fibroblasts from control individual, subject 1, and a subject with pathogenic *MRPS7* variants that were transduced with wild-type *MRPS34* cDNA. Complex I and complex IV activity was significantly increased in subject 1 cells transduced with wild-type *MRPS34* relative to untransduced cells (both $p < 0.0001$). Complex IV was significantly decreased in control individual cells transduced with wild-type *MRPS34* relative to untransduced cells ($p = 0.0004$). Results were normalized to citrate synthase and presented as the percent of average untransduced control cells. The data represents the mean of three independent transfections ± SEM.

(F) The level of small mitoribosomal subunit proteins MRPS5 and MRPS18B was examined in fibroblasts from control individuals (C1 and C2) and subject 4 transduced with either *RFP* or wild-type *MRPS34* by SDS-PAGE western blotting. Fibroblasts from subject 4 that had been transduced with wild-type *MRPS34* had increased levels of MRPS5 and MRPS18B relative to cells transduced with *RFP*. β-actin was used as a loading control. The blot shown is representative of three independent experiments.

MRPS34 mutations, together with our previous studies on the *Mrps34* mutant mouse,[18] show that MRPS34 defects lead to a significant decrease in all small mitoribosomal subunit proteins and significantly reduced 12S rRNA levels. These data suggest that MRPS34 plays an important role in stabilizing the 12S rRNA and is required for the stability of the small mitoribosomal subunit. The relative sparing of the large mitoribosomal subunit in MRPS34-deficient cells is consistent with studies examining cell lines from subjects with pathogenic mutations in other small mitoribosomal subunit proteins MRPS16 and MRPS22,[57] suggesting that the maintenance of large and small mitoribosomal subunit levels are not inextricably linked in humans. While the identification of affected subjects with pathogenic mutations in mitoribosomal subunit proteins enables key insight into mitoribosome stability, more comprehensive studies are required to enable an intimate understanding of mitochondrial ribosomes and protein synthesis.

Although complexes I, III, IV, and V all contain mtDNA-encoded subunits, our proteomic data suggest that complexes I and IV are more vulnerable than complexes III and V to destabilization when there is a defect in mitochondrial translation. We have previously shown that defective incorporation of mtDNA-encoded subunits into complexes I and IV can preclude assembly of these complexes, resulting in a general destabilization and turnover of unincorporated subunits.[40,42] Most of the mtDNA-encoded subunits of complexes I and IV that we detected in proteomic analyses of MRPS34-deficient fibroblasts appeared to be decreased. This was not the case for the MT-CYB and MT-ATP8 subunits of complexes III and V, suggesting that the lesser impact on complexes III and V may relate to longer half-lives of these proteins or their stabilization by association with other polypeptides within the assembled complex. Further studies are required to determine why different OXPHOS complexes are differentially impacted by a defect in mitochondrial translation.

The *Mrps34* mutant mouse showed similar defects in mitoribosome assembly and protein synthesis to the human disorder,[18] but the liver dysfunction that characterized that model was not a clinical feature of the six *MRPS34* disease subjects reported here. Further analyses of the *Mrps34* mutant mice have identified kidney dysfunction and smaller brains compared to controls (A.F., unpublished data), features seen in common with some of the subjects reported here. However, it remains to be determined why liver dysfunction was more prominent in *Mrps34* mutant mice. Mutations affecting mitochondrial translation machinery have often been associated with liver dysfunction.[8,11,58] The observed differences in presentation between individual patients and the mouse model may reflect the importance of both the location and severity of the mutation (including hypomorphic versus loss-of-function alleles) as well as the genetic background. This consideration is also relevant to the observed differences in both onset and progression of clinical disease between the different *MRPS34* human subjects.

In conclusion, our study demonstrates that MRPS34 is required for normal function of the mitoribosome and energy-generating mitochondrial OXPHOS system in humans. Autosomal-recessive splice site, missense, or nonsense mutations that destabilize MRPS34 are causal of clinical presentations of Leigh syndrome or a Leigh-like disease.

Accession Numbers

The ClinVar accession numbers for the *MRPS34* variants c.321+1G>T and c.37G>A are SCV000581390 and SCV000583446, respectively.

Supplemental Data

Supplemental Data include detailed Supplemental Note of case reports, seven tables, four figures, and a video and can be found with this article online at http://dx.doi.org/10.1016/j.ajhg.2017.07.005.

Conflicts of Interest

K.H., Z.Z., K.R., and R.B. are employees of GeneDx.

Acknowledgments

This project was supported by Australian National Health and Medical Research Council (NHMRC) fellowships and project grants to D.R.T., A.G.C., A.F., and D.A.S. (1022896, 1068409, 1068056, 1058442, 1078273, 1125390, 1107094, 1070916), the Australian Research Council (DP170103000 to A.F.), the Jaxson Flynt Research Fund (M.J.F. and J.B.), the Joseph and Pat Holveck Research Fund (M.J.F. and Z.Z.-C.), an Australian Postgraduate Award (N.J.L.), a NHMRC scholarship (1017174 to H.S.M.), Australian Mitochondrial Disease Foundation scholarship (N.J.L. and H.S.M.), the Victorian Government's Operational Infrastructure Support Program (D.R.T. and A.G.C.), the Icahn Institute for Genomics and Multiscale Biology, NIH National Institute of Child Health and Human Development (NICHD) (grant K08HD086827 to B.D.W.), the NIH (R01GM077465 and 1R35GM122455 to V.K.M.), the French Muscular Dystrophy Association (AFM grant #19876 to M.D.M.), and Genomit (01GML1207 to A.R.). We acknowledge the use of bioresources of the Necker Imagine DNA biobank (BB-033-00065). We thank the subjects, families, and multi-disciplinary clinical care providers for their involvement. The authors acknowledge the GeneMatcher tool, which enabled the identification of two of the families described in this study, and the Monash Biomedical Proteomics Facility, Monash University, for the provision of instrumentation, training, and technical support. We thank Associate Professor Susan Donath for her expert advice on appropriate statistical analyses. The content is solely the responsibility of the authors and does not necessarily represent the official views of the funding agencies.

Received: May 16, 2017
Accepted: July 9, 2017
Published: August 3, 2017

Web Resources

ClinVar, https://www.ncbi.nlm.nih.gov/clinvar/
dbSNP, http://www.ncbi.nlm.nih.gov/projects/SNP/
GenBank, http://www.ncbi.nlm.nih.gov/genbank/
GeneMatcher, https://genematcher.org/
gnomAD Browser, http://gnomad.broadinstitute.org/
MITOMAP, http://www.mitomap.org/MITOMAP
MSeqDR, https://mseqdr.org/
NHLBI Exome Sequencing Project (ESP) Exome Variant Server, http://evs.gs.washington.edu/EVS/
OMIM, http://www.omim.org/
RCSB Protein Data Bank, http://www.rcsb.org/pdb/home/home.do
Seqr, https://github.com/macarthur-lab/seqr

References

1. Ott, M., Amunts, A., and Brown, A. (2016). Organization and regulation of mitochondrial protein synthesis. Annu. Rev. Biochem. *85*, 77–101.
2. Mai, N., Chrzanowska-Lightowlers, Z.M., and Lightowlers, R.N. (2017). The process of mammalian mitochondrial protein synthesis. Cell Tissue Res. *367*, 5–20.
3. Greber, B.J., and Ban, N. (2016). Structure and function of the mitochondrial ribosome. Annu. Rev. Biochem. *85*, 103–132.
4. Greber, B.J., Boehringer, D., Leibundgut, M., Bieri, P., Leitner, A., Schmitz, N., Aebersold, R., and Ban, N. (2014). The complete structure of the large subunit of the mammalian mitochondrial ribosome. Nature *515*, 283–286.
5. Greber, B.J., Bieri, P., Leibundgut, M., Leitner, A., Aebersold, R., Boehringer, D., and Ban, N. (2015). Ribosome. The complete structure of the 55S mammalian mitochondrial ribosome. Science *348*, 303–308.
6. Rorbach, J., Gao, F., Powell, C.A., D'Souza, A., Lightowlers, R.N., Minczuk, M., and Chrzanowska-Lightowlers, Z.M. (2016). Human mitochondrial ribosomes can switch their structural RNA composition. Proc. Natl. Acad. Sci. USA *113*, 12198–12201.

7. Boczonadi, V., and Horvath, R. (2014). Mitochondria: impaired mitochondrial translation in human disease. Int. J. Biochem. Cell Biol. *48*, 77–84.
8. Menezes, M.J., Guo, Y., Zhang, J., Riley, L.G., Cooper, S.T., Thorburn, D.R., Li, J., Dong, D., Li, Z., Glessner, J., et al. (2015). Mutation in mitochondrial ribosomal protein S7 (MRPS7) causes congenital sensorineural deafness, progressive hepatic and renal failure and lactic acidemia. Hum. Mol. Genet. *24*, 2297–2307.
9. Miller, C., Saada, A., Shaul, N., Shabtai, N., Ben-Shalom, E., Shaag, A., Hershkovitz, E., and Elpeleg, O. (2004). Defective mitochondrial translation caused by a ribosomal protein (MRPS16) mutation. Ann. Neurol. *56*, 734–738.
10. Saada, A., Shaag, A., Arnon, S., Dolfin, T., Miller, C., Fuchs-Telem, D., Lombes, A., and Elpeleg, O. (2007). Antenatal mitochondrial disease caused by mitochondrial ribosomal protein (MRPS22) mutation. J. Med. Genet. *44*, 784–786.
11. Kohda, M., Tokuzawa, Y., Kishita, Y., Nyuzuki, H., Moriyama, Y., Mizuno, Y., Hirata, T., Yatsuka, Y., Yamashita-Sugahara, Y., Nakachi, Y., et al. (2016). A comprehensive genomic analysis reveals the genetic landscape of mitochondrial respiratory chain complex deficiencies. PLoS Genet. *12*, e1005679.
12. Galmiche, L., Serre, V., Beinat, M., Assouline, Z., Lebre, A.S., Chretien, D., Nietschke, P., Benes, V., Boddaert, N., Sidi, D., et al. (2011). Exome sequencing identifies MRPL3 mutation in mitochondrial cardiomyopathy. Hum. Mutat. *32*, 1225–1231.
13. Serre, V., Rozanska, A., Beinat, M., Chretien, D., Boddaert, N., Munnich, A., Rötig, A., and Chrzanowska-Lightowlers, Z.M. (2013). Mutations in mitochondrial ribosomal protein MRPL12 leads to growth retardation, neurological deterioration and mitochondrial translation deficiency. Biochim. Biophys. Acta *1832*, 1304–1312.
14. Carroll, C.J., Isohanni, P., Pöyhönen, R., Euro, L., Richter, U., Brilhante, V., Götz, A., Lahtinen, T., Paetau, A., Pihko, H., et al. (2013). Whole-exome sequencing identifies a mutation in the mitochondrial ribosome protein MRPL44 to underlie mitochondrial infantile cardiomyopathy. J. Med. Genet. *50*, 151–159.
15. Bursle, C., Narendra, A., Chuk, R., Cardinal, J., Justo, R., Lewis, B., and Coman, D. (2017). COXPD9 an evolving multisystem disease; congenital lactic acidosis, sensorineural hearing loss, hypertrophic cardiomyopathy, cirrhosis and interstitial nephritis. JIMD Rep. *34*, 105–109.
16. Distelmaier, F., Haack, T.B., Catarino, C.B., Gallenmüller, C., Rodenburg, R.J., Strom, T.M., Baertling, F., Meitinger, T., Mayatepek, E., Prokisch, H., and Klopstock, T. (2015). MRPL44 mutations cause a slowly progressive multisystem disease with childhood-onset hypertrophic cardiomyopathy. Neurogenetics *16*, 319–323.
17. Arroyo, J.D., Jourdain, A.A., Calvo, S.E., Ballarano, C.A., Doench, J.G., Root, D.E., and Mootha, V.K. (2016). A genome-wide CRISPR death screen identifies genes essential for oxidative phosphorylation. Cell Metab. *24*, 875–885.
18. Richman, T.R., Ermer, J.A., Davies, S.M., Perks, K.L., Viola, H.M., Shearwood, A.M., Hool, L.C., Rackham, O., and Filipovska, A. (2015). Mutation in MRPS34 compromises protein synthesis and causes mitochondrial dysfunction. PLoS Genet. *11*, e1005089.
19. Lake, N.J., Compton, A.G., Rahman, S., and Thorburn, D.R. (2016). Leigh syndrome: One disorder, more than 75 monogenic causes. Ann. Neurol. *79*, 190–203.
20. Frazier, A.E., and Thorburn, D.R. (2012). Biochemical analyses of the electron transport chain complexes by spectrophotometry. Methods Mol. Biol. *837*, 49–62.
21. Rustin, P., Chretien, D., Bourgeron, T., Gérard, B., Rötig, A., Saudubray, J.M., and Munnich, A. (1994). Biochemical and molecular investigations in respiratory chain deficiencies. Clin. Chim. Acta *228*, 35–51.
22. Calvo, S.E., Compton, A.G., Hershman, S.G., Lim, S.C., Lieber, D.S., Tucker, E.J., Laskowski, A., Garone, C., Liu, S., Jaffe, D.B., et al. (2012). Molecular diagnosis of infantile mitochondrial disease with targeted next-generation sequencing. Sci. Transl. Med. *4*, 118ra10.
23. Li, H., and Durbin, R. (2009). Fast and accurate short read alignment with Burrows-Wheeler transform. Bioinformatics *25*, 1754–1760.
24. McKenna, A., Hanna, M., Banks, E., Sivachenko, A., Cibulskis, K., Kernytsky, A., Garimella, K., Altshuler, D., Gabriel, S., Daly, M., and DePristo, M.A. (2010). The Genome Analysis Toolkit: a MapReduce framework for analyzing next-generation DNA sequencing data. Genome Res. *20*, 1297–1303.
25. Van der Auwera, G.A., Carneiro, M.O., Hartl, C., Poplin, R., Del Angel, G., Levy-Moonshine, A., Jordan, T., Shakir, K., Roazen, D., Thibault, J., et al. (2013). From FastQ data to high confidence variant calls: the Genome Analysis Toolkit best practices pipeline. Curr. Protoc. Bioinformatics *43*, 1–33.
26. DePristo, M.A., Banks, E., Poplin, R., Garimella, K.V., Maguire, J.R., Hartl, C., Philippakis, A.A., del Angel, G., Rivas, M.A., Hanna, M., et al. (2011). A framework for variation discovery and genotyping using next-generation DNA sequencing data. Nat. Genet. *43*, 491–498.
27. McLaren, W., Gil, L., Hunt, S.E., Riat, H.S., Ritchie, G.R., Thormann, A., Flicek, P., and Cunningham, F. (2016). The Ensembl Variant Effect Predictor. Genome Biol. *17*, 122.
28. Lieber, D.S., Calvo, S.E., Shanahan, K., Slate, N.G., Liu, S., Hershman, S.G., Gold, N.B., Chapman, B.A., Thorburn, D.R., Berry, G.T., et al. (2013). Targeted exome sequencing of suspected mitochondrial disorders. Neurology *80*, 1762–1770.
29. Retterer, K., Juusola, J., Cho, M.T., Vitazka, P., Millan, F., Gibellini, F., Vertino-Bell, A., Smaoui, N., Neidich, J., Monaghan, K.G., et al. (2016). Clinical application of whole-exome sequencing across clinical indications. Genet. Med. *18*, 696–704.
30. Webb, B.D., Metikala, S., Wheeler, P.G., Sherpa, M.D., Houten, S.M., Horb, M.E., and Schadt, E.E. (2017). Heterozygous pathogenic variant in DACT1 causes an autosomal-dominant syndrome with features overlapping Townes-Brocks syndrome. Hum. Mutat. *38*, 373–377.
31. Vedrenne, V., Gowher, A., De Lonlay, P., Nitschke, P., Serre, V., Boddaert, N., Altuzarra, C., Mager-Heckel, A.M., Chretien, F., Entelis, N., et al. (2012). Mutation in PNPT1, which encodes a polyribonucleotide nucleotidyltransferase, impairs RNA import into mitochondria and causes respiratory-chain deficiency. Am. J. Hum. Genet. *91*, 912–918.
32. Calvo, S.E., Tucker, E.J., Compton, A.G., Kirby, D.M., Crawford, G., Burtt, N.P., Rivas, M., Guiducci, C., Bruno, D.L., Goldberger, O.A., et al. (2010). High-throughput, pooled sequencing identifies mutations in NUBPL and FOXRED1 in human complex I deficiency. Nat. Genet. *42*, 851–858.
33. Cooper, S.T., Lo, H.P., and North, K.N. (2003). Single section Western blot: improving the molecular diagnosis of the muscular dystrophies. Neurology *61*, 93–97.

34. Johnston, A.J., Hoogenraad, J., Dougan, D.A., Truscott, K.N., Yano, M., Mori, M., Hoogenraad, N.J., and Ryan, M.T. (2002). Insertion and assembly of human tom7 into the preprotein translocase complex of the outer mitochondrial membrane. J. Biol. Chem. *277*, 42197–42204.
35. Wittig, I., Braun, H.P., and Schägger, H. (2006). Blue native PAGE. Nat. Protoc. *1*, 418–428.
36. Sánchez-Caballero, L., Ruzzenente, B., Bianchi, L., Assouline, Z., Barcia, G., Metodiev, M.D., Rio, M., Funalot, B., van den Brand, M.A., Guerrero-Castillo, S., et al. (2016). Mutations in complex I assembly factor TMEM126B result in muscle weakness and isolated complex I deficiency. Am. J. Hum. Genet. *99*, 208–216.
37. Rackham, O., Davies, S.M., Shearwood, A.M., Hamilton, K.L., Whelan, J., and Filipovska, A. (2009). Pentatricopeptide repeat domain protein 1 lowers the levels of mitochondrial leucine tRNAs in cells. Nucleic Acids Res. *37*, 5859–5867.
38. Richman, T.R., Spåhr, H., Ermer, J.A., Davies, S.M., Viola, H.M., Bates, K.A., Papadimitriou, J., Hool, L.C., Rodger, J., Larsson, N.G., et al. (2016). Loss of the RNA-binding protein TACO1 causes late-onset mitochondrial dysfunction in mice. Nat. Commun. *7*, 11884.
39. McKenzie, M., Lazarou, M., Thorburn, D.R., and Ryan, M.T. (2007). Analysis of mitochondrial subunit assembly into respiratory chain complexes using Blue Native polyacrylamide gel electrophoresis. Anal. Biochem. *364*, 128–137.
40. Stroud, D.A., Maher, M.J., Lindau, C., Vögtle, F.N., Frazier, A.E., Surgenor, E., Mountford, H., Singh, A.P., Bonas, M., Oeljeklaus, S., et al. (2015). COA6 is a mitochondrial complex IV assembly factor critical for biogenesis of mtDNA-encoded COX2. Hum. Mol. Genet. *24*, 5404–5415.
41. Sasarman, F., and Shoubridge, E.A. (2012). Radioactive labeling of mitochondrial translation products in cultured cells. Methods Mol. Biol. *837*, 207–217.
42. Stroud, D.A., Surgenor, E.E., Formosa, L.E., Reljic, B., Frazier, A.E., Dibley, M.G., Osellame, L.D., Stait, T., Beilharz, T.H., Thorburn, D.R., et al. (2016). Accessory subunits are integral for assembly and function of human mitochondrial complex I. Nature *538*, 123–126.
43. Kulak, N.A., Pichler, G., Paron, I., Nagaraj, N., and Mann, M. (2014). Minimal, encapsulated proteomic-sample processing applied to copy-number estimation in eukaryotic cells. Nat. Methods *11*, 319–324.
44. Tyanova, S., Temu, T., and Cox, J. (2016). The MaxQuant computational platform for mass spectrometry-based shotgun proteomics. Nat. Protoc. *11*, 2301–2319.
45. Tyanova, S., Temu, T., Sinitcyn, P., Carlson, A., Hein, M.Y., Geiger, T., Mann, M., and Cox, J. (2016). The Perseus computational platform for comprehensive analysis of (prote)omics data. Nat. Methods *13*, 731–740.
46. Calvo, S.E., Clauser, K.R., and Mootha, V.K. (2016). MitoCarta2.0: an updated inventory of mammalian mitochondrial proteins. Nucleic Acids Res. *44* (D1), D1251–D1257.
47. Zhu, J., Vinothkumar, K.R., and Hirst, J. (2016). Structure of mammalian respiratory complex I. Nature *536*, 354–358.
48. Amunts, A., Brown, A., Toots, J., Scheres, S.H., and Ramakrishnan, V. (2015). Ribosome. The structure of the human mitochondrial ribosome. Science *348*, 95–98.
49. Iwata, S., Lee, J.W., Okada, K., Lee, J.K., Iwata, M., Rasmussen, B., Link, T.A., Ramaswamy, S., and Jap, B.K. (1998). Complete structure of the 11-subunit bovine mitochondrial cytochrome bc1 complex. Science *281*, 64–71.
50. Yano, N., Muramoto, K., Shimada, A., Takemura, S., Baba, J., Fujisawa, H., Mochizuki, M., Shinzawa-Itoh, K., Yamashita, E., Tsukihara, T., and Yoshikawa, S. (2016). The Mg2+-containing water cluster of mammalian cytochrome c oxidase collects four pumping proton equivalents in each catalytic cycle. J. Biol. Chem. *291*, 23882–23894.
51. Sun, F., Huo, X., Zhai, Y., Wang, A., Xu, J., Su, D., Bartlam, M., and Rao, Z. (2005). Crystal structure of mitochondrial respiratory membrane protein complex II. Cell *121*, 1043–1057.
52. Lek, M., Karczewski, K.J., Minikel, E.V., Samocha, K.E., Banks, E., Fennell, T., O'Donnell-Luria, A.H., Ware, J.S., Hill, A.J., Cummings, B.B., et al.; Exome Aggregation Consortium (2016). Analysis of protein-coding genetic variation in 60,706 humans. Nature *536*, 285–291.
53. Sherry, S.T., Ward, M.H., Kholodov, M., Baker, J., Phan, L., Smigielski, E.M., and Sirotkin, K. (2001). dbSNP: the NCBI database of genetic variation. Nucleic Acids Res. *29*, 308–311.
54. Sobreira, N., Schiettecatte, F., Valle, D., and Hamosh, A. (2015). GeneMatcher: a matching tool for connecting investigators with an interest in the same gene. Hum. Mutat. *36*, 928–930.
55. Diodato, D., Ghezzi, D., and Tiranti, V. (2014). The mitochondrial aminoacyl tRNA synthetases: genes and syndromes. Int. J. Cell Biol. *2014*, 787956.
56. Mayr, J.A., Haack, T.B., Freisinger, P., Karall, D., Makowski, C., Koch, J., Feichtinger, R.G., Zimmermann, F.A., Rolinski, B., Ahting, U., et al. (2015). Spectrum of combined respiratory chain defects. J. Inherit. Metab. Dis. *38*, 629–640.
57. Emdadul Haque, M., Grasso, D., Miller, C., Spremulli, L.L., and Saada, A. (2008). The effect of mutated mitochondrial ribosomal proteins S16 and S22 on the assembly of the small and large ribosomal subunits in human mitochondria. Mitochondrion *8*, 254–261.
58. Sasarman, F., Nishimura, T., Antonicka, H., Weraarpachai, W., Shoubridge, E.A.; and LSFC Consortium (2015). Tissue-specific responses to the LRPPRC founder mutation in French Canadian Leigh Syndrome. Hum. Mol. Genet. *24*, 480–491.

The American Journal of Human Genetics, Volume *101*

Supplemental Data

Biallelic Mutations in *MRPS34* Lead to Instability of the Small Mitoribosomal Subunit and Leigh Syndrome

Nicole J. Lake, Bryn D. Webb, David A. Stroud, Tara R. Richman, Benedetta Ruzzenente, Alison G. Compton, Hayley S. Mountford, Juliette Pulman, Coralie Zangarelli, Marlene Rio, Nathalie Bodaert, Zahra Assouline, Mingma D. Sherpa, Eric E. Schadt, Sander M. Houten, James Byrnes, Elizabeth M. McCormick, Zarazuela Zolkipli-Cunningham, Katrina Haude, Zhancheng Zhang, Kyle Retterer, Renkui Bai, Sarah E. Calvo, Vamsi K. Mootha, John Christodoulou, Agnes Rötig, Aleksandra Filipovska, Ingrid Cristian, Marni J. Falk, Metodi D. Metodiev, and David R. Thorburn

Supplemental Data

Supplemental Note: Case Reports.

Subject 1 (Figure 1A family 1 subject II-3) was the third child of double first cousin parents of Italian ancestry living in Australia. The pregnancy was complicated by an elevated serum maternal alphafetoprotein, with a normal male karyotype being identified at amniocentesis. He was born at 42 weeks gestation by an induced delivery. He was in good condition at birth, and had no postnatal problems. Head growth was noted to be slowed from 2 months of age. He first came to medical attention at 4 months of age because of developmental delay and microcephaly. A CT scan of the head at that time was reported as normal. Other investigations at that time did not suggest a potential etiology. At 6 months of age he first developed marked irritability and episodes of stiffening. At 8 months of age he became very drowsy and lethargic, not associated with any intercurrent illness or change in his diet, which was initially intermittent, but subsequently became continuous and was associated with poor feeding. At this time he was noted to have episodic tachypnoea, lasting minutes at a time, and blood lactate was 4.2 mmol/L (normal range 0.7 – 2.0) and CSF lactate was 8.9 mmol/L (normal < 2). An initial urine amino and organic acid screen was normal, with a repeat study showing raised alanine levels. A trial of coenzyme Q, riboflavin and vitamin K appeared of no obvious benefit. At 9 months of age he suddenly deteriorated with gasping respirations, and became cyanosed. Despite vigorous attempts at resuscitation by ambulance staff and at a tertiary hospital he could not be revived. Muscle collected five hours after death showed a predominance of Type 1 fibers. Routine mitochondrial stains were normal, with no ragged red fibers noted. However, combined COX/SDH staining showed a diffuse pattern suggestive of cytochrome c oxidase deficiency. Similar results were seen with combined COX/NADH-TR staining. Post mortem examination of the brain revealed changes typical of Leigh syndrome, with symmetrical changes including rarefied neuropil, vascular proliferation and gliosis. Affected areas included the central part of the medulla oblongata, vestibular nuclei and olives, and the tegmentum of the pons, with extension into the inferior cerebellar peduncles, much of the midbrain, the basal ganglia and the thalami. His two older sisters are clinically normal. There is a maternal first cousin (parents were not consanguineous) who died of spinal muscular atrophy type 1. Prenatal testing, based on measuring OXPHOS enzymes in cultured

chorionic villus cells, was performed for a pregnancy three years after the death of the proband, and predicted that the fetus would not be affected. A male infant (Figure 1A family 1 subject II-4) was subsequently born, with subsequent growth and development reported as normal.

Subject 2a (Figure 1 A, family 2 subject II-1) is a 17-year old female of Puerto Rican descent born at full-term by spontaneous vaginal delivery. Birth weight was 2.55 kg, length was 46 cm, and head circumference was 32.4 cm. She had a routine newborn hospital stay and was discharged home at 2 days of age. She breastfed without difficulty for 6 months. Hypotonia was noted by 6 months of age. By 9-10 months of age, lack of developmental progress was noted, and the patient was evaluated by a neurologist who diagnosed motor delay. Ophthalmologic evaluation at 10 months disclosed lacrimal duct blockage, but no other abnormalities. At 12 months, occasional exotropia was noted, which became constant by 13 months of age and ptosis developed by 15 months. Tremors were first noted at 10 months of age, and increased spasticity was noted by 1 year. Initial brain MRI without contrast was normal at 11 months of age. Repeat brain MRI with and without contrast, completed at age 1 year 8 months, revealed abnormal bright T2 and FLAIR signal in the posterior half of the midbrain with extension to the quadrigeminal plate. The abnormal signal extended to the posterior portion of the pons, abutting the floor of the 4th ventricle. Small areas of increased T2 and FLAIR signal were seen in both cerebral peduncles at the level of the midbrain. MR spectroscopy showed a normal lactate peak on left basal ganglia at 4 years of age. Multiple other brain MRIs without contrast were normal (2 years 5 months, 4 years, and 11 years of age). Extensive workup was performed including two muscle biopsies before whole exome sequencing was completed. The first muscle biopsy was at 19 months of age, which was reported as normal, including normal electron transfer chain (ETC) studies. The second muscle biopsy was performed at 12 years of age which showed normal quantitative western blot ETC subunits and normal mitochondrial depletion studies, but decreased complex I, III and IV enzyme activities. Serum lactate levels showed intermittent mild elevation and CSF lactate measured at age 14 years 2 months was 3.5 mmol/L (reference range 1.1-2.8 mmol/L). Other workup included normal metabolic workup (urine amino acids, urine organic acids, plasma amino acids, carnitine, pyruvate, acylcarnitine profile in plasma and in fibroblasts, leukocyte CoQ10, creatine and

GAA studies, isoelectric focusing for CDGs, CMP, vitamin E, succinyladenosine), CPK, lysosomal enzymes, CSF testing (amino acids, sialic acid, neurotransmitters, organic acids), FISH studies for PWS/Angelman syndrome and molecular testing (mtDNA sequencing/deletion/duplication, *MECP2, UBE3A, CDKL5, ARX, PLA2G6* gene sequencing). 5-methyltetrahydrofolate level in CSF was mildly decreased. EEG was normal at 27 months of age. Other past medical history includes a horseshoe kidney diagnosed incidentally. Past surgical history is notable for strabismus surgery and scoliosis correction. She met some normal motor developmental milestones including rolling over on time. She was able to sit at 9 months and cruise at 12 months. She lost these skills slowly over time. She is currently in a wheelchair. She is nonverbal, but engages socially with facial expressions including a social smile. She can fix vision on objects and can follow some simple commands with hands. On the most recent exam, at age 17 years, the patient sits upright in a wheelchair, but has dystonic movements of her trunk. Head circumference is 50 cm (8 SD below mean), weight is 34.3 kg (5 SD below mean) and length is 144.8 cm (2 SD below mean). She has microcephaly and mild coarsening of features with thick eyebrows. The anterior hairline extends onto her forehead. She is able to move her head and has normal extraocular movements with intermittent strabismus. She has normal nose, mouth and ears. Chest exam is significant for kyphoscoliosis. Cardiovascular and respiratory exams are normal. Abdomen is not distended, with no hepatosplenomegaly. Her sexual development is Tanner stage V, normal female. Extremities are atrophic and with significant hypertonia, more evident on left side compared to right. Mild contractures are seen in most joints. She has bilateral choreoathetoid movements, which increase with agitation, but she is able to try to grab objects with overshooting. Reflexes are 4+ throughout.

Subject 2b (Figure 1A family 2 subject II-2), sibling of subject 2a, is a 14-year old female and is similarly affected with global developmental delay, regression, microcephaly, and a choreoathetoid spastic quadriplegia. She was born at 37 weeks gestation by normal spontaneous vaginal delivery. Birth weight was 1.99 kg. She had a normal neonatal hospital stay and was discharged home at 2 days of age. Developmental milestones included the ability to roll over at 8 months of age, sit alone at 12 months of age, crawl at 8-10 months, cruise at 9-11 months, and walk at 15 months. On review of her

medical history, she had a gastrostomy tube placed in the last 2 years due to aspiration pneumonia. She had surgery for strabismus. From an orthopedic standpoint, she had a femur fracture and required a femoral shaft osteotomy as well as tendon lengthening and scoliosis surgery. There are no cardiac abnormalities, and no hearing impairment is suspected. MRI of brain without contrast at 9 years of age showed mild cerebellar atrophy, otherwise unremarkable. There is no history of seizures. She has had a workup, but less extensive than her sister. She has not had a muscle biopsy, CSF studies, or a skin biopsy. Serum lactate levels showed intermittent mild elevation. Normal studies include metabolic (urine amino acids, urine organic acids, plasma amino acids, carnitine, pyruvate, acylcarnitine profile, very long chain fatty acids, leukocyte CoQ10, isoelectric focusing for a congenital disorder of glycosylation, a comprehensive metabolic panel (CMP) and vitamin E), CPK, lysosomal enzymes, karyotype, subtelomeric FISH, molecular testing (microarray and Fragile X). EEG was normal at 8 years of age. She is nonverbal, social, and uses signs and assistive devices to communicate. She has demonstrated mastery of colors, numbers, and letters with the use of assistive devices. On examination at 13 years of age, weight was 26.5 kg (4SD below the mean), length is difficult to assess due to dystonia but was 137.2 cm (3SD below the mean) and head circumference was 50.6 cm (8SD below the mean). She is microcephalic with mild coarsening of facial features. Her forehead is small with the anterior hairline extending onto forehead. She has thick eyebrows. She has normal extraocular movements with normal nose, mouth and ears, except for larger size ears. Chest exam reveals that she too had kyphoscoliosis. Cardiovascular and respiratory exam are normal. Abdomen is not distended without hepatosplenomegaly. Tanner stage V, normal female. Extremities are atrophic and with increased startle response. Mild contractures are seen in many joints. She has bilateral choreoathetoid movements but less than her sister. Reflexes are 3+ throughout.

Subject 3a (Figure 1A family 3 subject II-1) is also of Puerto Rican ancestry and was born at 39 weeks gestation with birth weight 3.43 kg and birth length 52 cm. Prenatal ultrasounds were reportedly normal, delivery was vaginal, and there were no complications or birth defects. Nystagmus was transiently noted at age six months, and recurred at 16 months. She developed generalized, rhythmic, involuntary movements of her extremities at 6 months of age, with normal EEG. Hypotonia

was noted at 7 months. She rolled over at 2-3 months, sat unassisted at 6-7 months, pulled to stand and had five words at 12 months, but experienced developmental regression, vomiting and weight loss at 20 months at which time she lost expressive speech and all motor milestones including head control and visual perception. Review of systems is significant for constipation noted at 16 months. NG feeds were initiated due to aspiration/inability to tolerate liquids by mouth as noted on a swallow study at 22 months of age. Gastrostomy tube was placed at 23 months of age. Now aged 7 years, she is non-ambulatory, wheelchair dependent, and non-verbal. Neurologic abnormalities on exam include axial hypotonia, limb hypertonia, hyperreflexia, and flexion contractures at the knees and ankles. She has large amplitude, hyperkinetic movements mainly in her upper extremities. Ophthalmologic concerns include optic atrophy identified at 3 years of age, central vision loss and primary use of peripheral vision with apparent up-gaze mobility impairment, intermittent ptosis, and alternating exotropia. She has poor sleep with suspected sleep apnea. She has precocious adrenarche and slightly advanced bone age. Audiogram studies performed at 2.5 years of age were unrevealing. Dysmorphic facies noted include a high and narrow palate that is V-shaped anteriorly, thick gums, short columella, and mild synophrys. EKG and echocardiogram were normal. Family history is noncontributory. Brain MRI at 20 months showed abnormal FLAIR/T2 hyperintensity and restricted diffusion involving the medial thalami and periaqueductal gray matter. Repeat brain MRI at 5 years showed symmetric mild thalamic atrophy with gliosis, periventricular white matter gliosis, and prominent lateral ventricles. Brain MRS was normal. Muscle biopsy at 21 months showed mild to moderate atrophy of type II fibers, and to a lesser extent type I fibers; patchy increase in subsarcolemmal NADH-TR and COX staining; mild increase in subsarcolemmal mitochondria and mitochondria-associated lipid vacuoles on electron microscopy; and complex I-III, II-III, and II deficiency with secondary mitochondrial proliferation as evidenced by elevated citrate synthase (154% of normal). Mitochondrial DNA sequencing by next-generation sequencing in blood and muscle revealed a nearly homoplasmic rare variant, m.15287T>C. This variant (MT-CYB, p.Phe181Leu) has only been tenuously linked to disease, with a single report describing a possible but unclear link with non-syndromic hearing loss.[1] Mitochondrial DNA content in muscle was normal at approximately 113% of the mean value of age- and tissue-matched controls. Biochemical testing revealed mildly elevated lactate (2.6 mmol/L; normal <2.2 mmol/L) and

decreased ammonia. Pyruvate, lactate/pyruvate ratio, plasma amino acid analysis, plasma carnitine analysis, acylcarnitine profile, leukocyte CoQ10 level, urine organic acid analysis, urine amino acid analysis, and urine orotic acid concentration were all unrevealing. Sequencing of 101 known primary mitochondrial disease genes, a sequencing panel of 77 genes associated with Leigh syndrome, and a genome-wide SNP microarray were normal.

Subject 3b (Figure 1A family 3 subject II-2) is the younger sister of subject 3a, and was born at 34 weeks gestation following induction of labor for spontaneous premature rupture of membranes at 21 weeks' and concern for oligohydramnios. Birth weight was 2.3 kg and birth length was 48 cm. She remained in the NICU for three weeks. She presented with mild developmental delay in her motor skills at 6 months and delay in her expressive language skills at 12 months, as well as dysconjugate eye movements at 13 months. She sat unassisted at 10 months, crawled at 15 months, and at 2 years of age, has not achieved independent walking and has limited language development. Review of systems is significant for dysphagia at 23 months with confirmed micro-aspiration on a barium swallow study. Now aged 2 years, neurologic abnormalities on exam include symmetric, exaggerated knee deep-tendon reflexes, dysconjugate eye movements with no ptosis, and tremulous head movements. She has not experienced developmental regression. Ophthalmologic concerns include limited right eye elevation and adduction deficit. She has poor sleep with pauses in breathing with suspected sleep apnea. Audiology testing has not been performed. She is nondysmorphic. Echocardiogram and EKG were normal. Brain MRI at 18 months revealed bilateral symmetric foci of T2 hyperintensity and restricted diffusion in the medulla, restiform bodies, and midbrain. Brain MRS was normal. EEG performed at 10 months was normal. Muscle biopsy was not performed. Biochemical testing revealed mildly elevated lactate (2.9 mM, normal < 2.0 mM). Pyruvate, lactate/pyruvate ratio, plasma amino acid analysis, plasma carnitine analysis, acylcarnitine profile, ammonia, creatine kinase, urine organic acid analysis, and urine amino acid analysis were all unrevealing.

Subject 4 (Figure 1A family 4 subject II-1) was a French boy, first child of healthy and non-consanguineous parents with no relevant family history. Pregnancy was marked by maternal

hypertension. He was born at term by cesarean section for fetal distress, but did not require neonatal resuscitation. Birth parameters were normal (Birth weight 2.99 kg, Length 51 cm, head circumference 34 cm). During the first weeks of life, he fed poorly and gained weight slowly, partly due to gastro-esophageal reflux. He had poor eye contact at 1 month of age. He could smile at 2 months and hold up his head at 4 months, but progressively lost these skills. At 6 months, weight was 6.02 kg (-2SD), height 64 cm (-1SD), head circumference 41 cm (-2SD). Examination showed no ocular contact, axial hypotonia, pyramidal syndrome of the lower limbs, and dystonia. Ophthalmologic examination was normal. Brain-MRI revealed the typical lesions in the brainstem observed in Leigh syndrome. He presented with two events of hemodynamic instability related to tubulopathy. During these episodes, laboratory investigation revealed transient metabolic acidosis, with elevated lactate levels of 3.0 mmol/L in plasma and 3.0 mmol/L in CSF. Muscle biopsy study revealed lipidosis and low complex IV activity. He died at 8.5 months of age from respiratory distress.

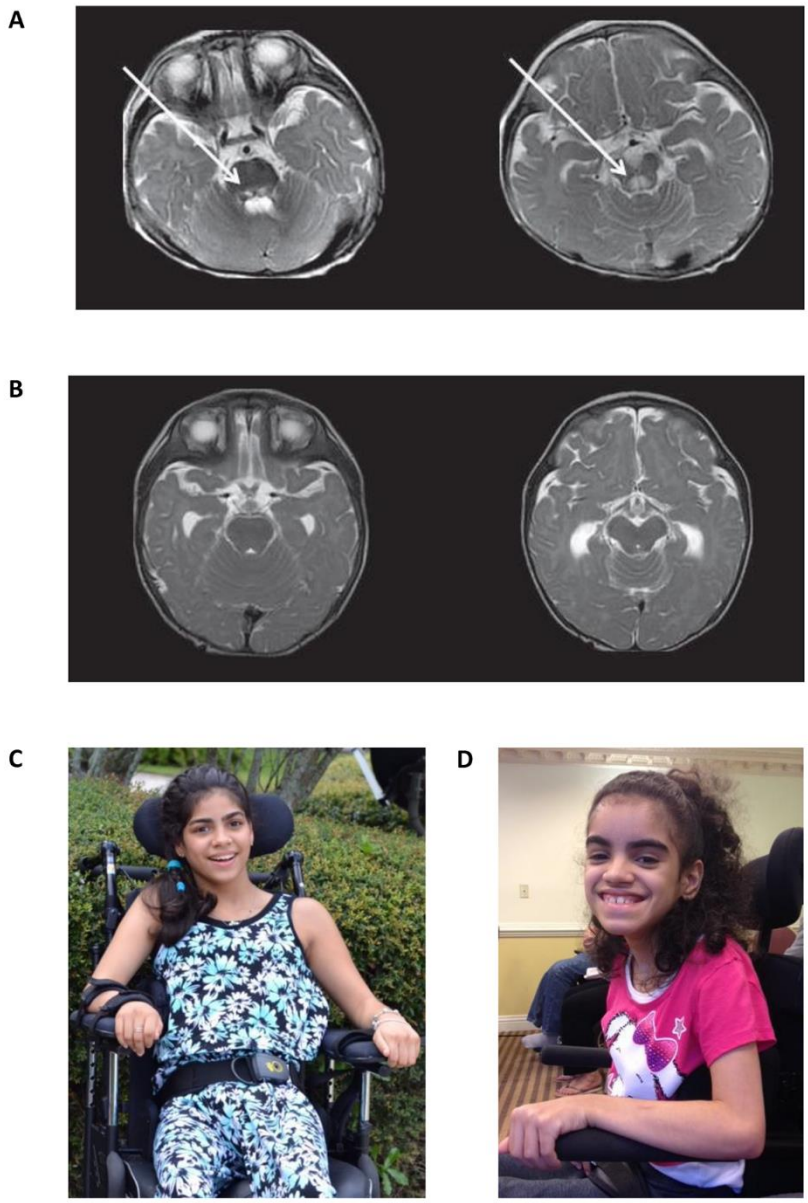

Figure S1. Neuropathology and patient images.

(A and B) Brain MRI of subject 4 (A) and an age-matched control (B) at 6 months of age. Axial, T2 weighted image shows bilateral abnormal hyperintensities in the brainstem, mainly in the dorsal brainstem nuclei (left arrow) and in periaqueductal region (right arrow), in subject 4.
(C and D) Subject 2a at 17 years of age and 2b at 12 years of age.

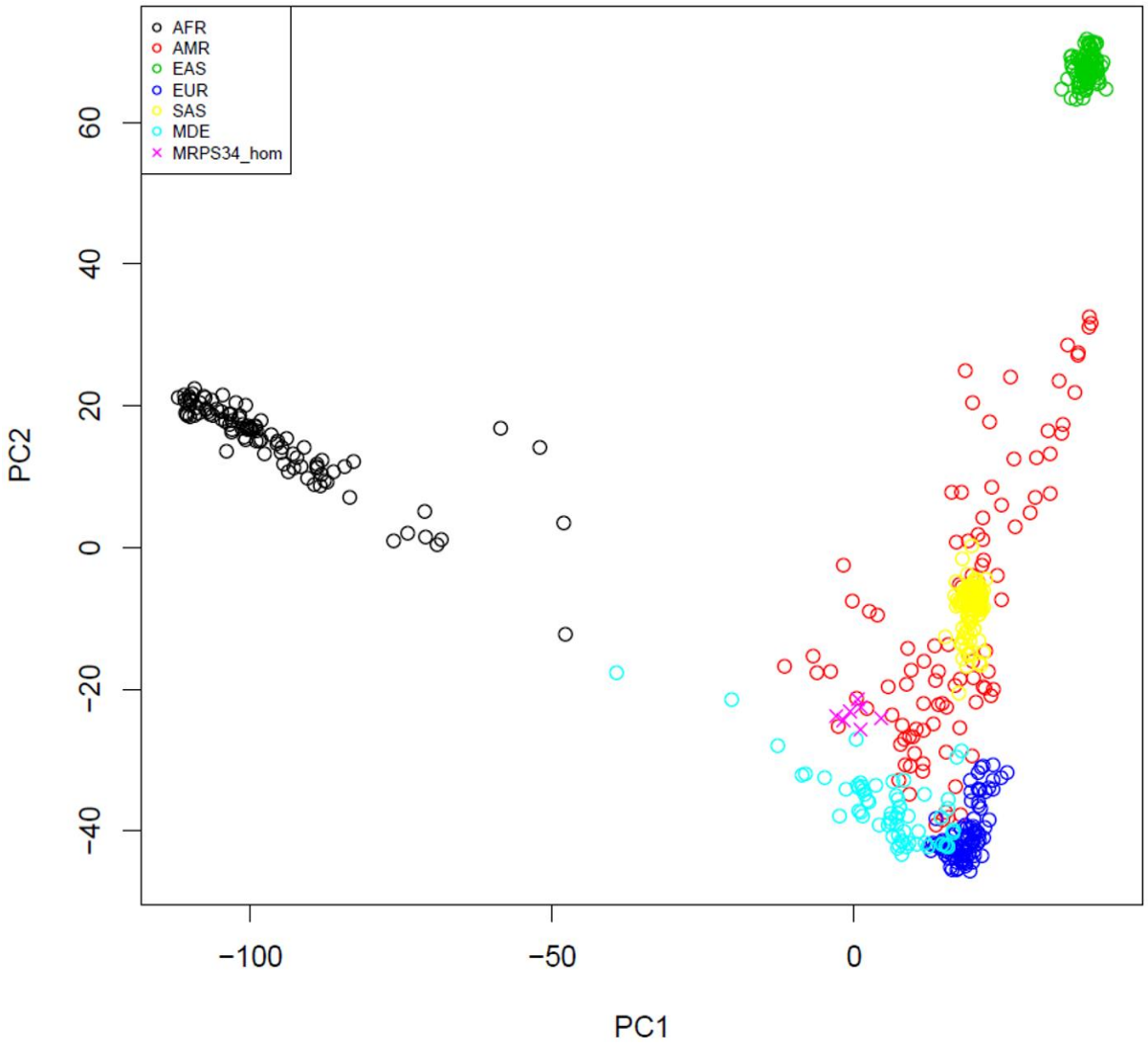

Figure S2. Principal Component Analysis of exome SNP genotypes from families 2 and 3 compared against 100 representative samples of each of the major 1000 Genomes Project Phase 3 populations (African [AFR], Admixed American [AMR], East Asian [EAS], European [EUR], and South Asian [SAS]) plus 61 GeneDx-sequenced samples with a known population origin of Middle Eastern (MDE). Five total components were calculated (see Table S3) but only the two most informative components (PC1 and PC2) are shown. "MRPS34_hom" refers to subjects and parents from families 2 and 3.

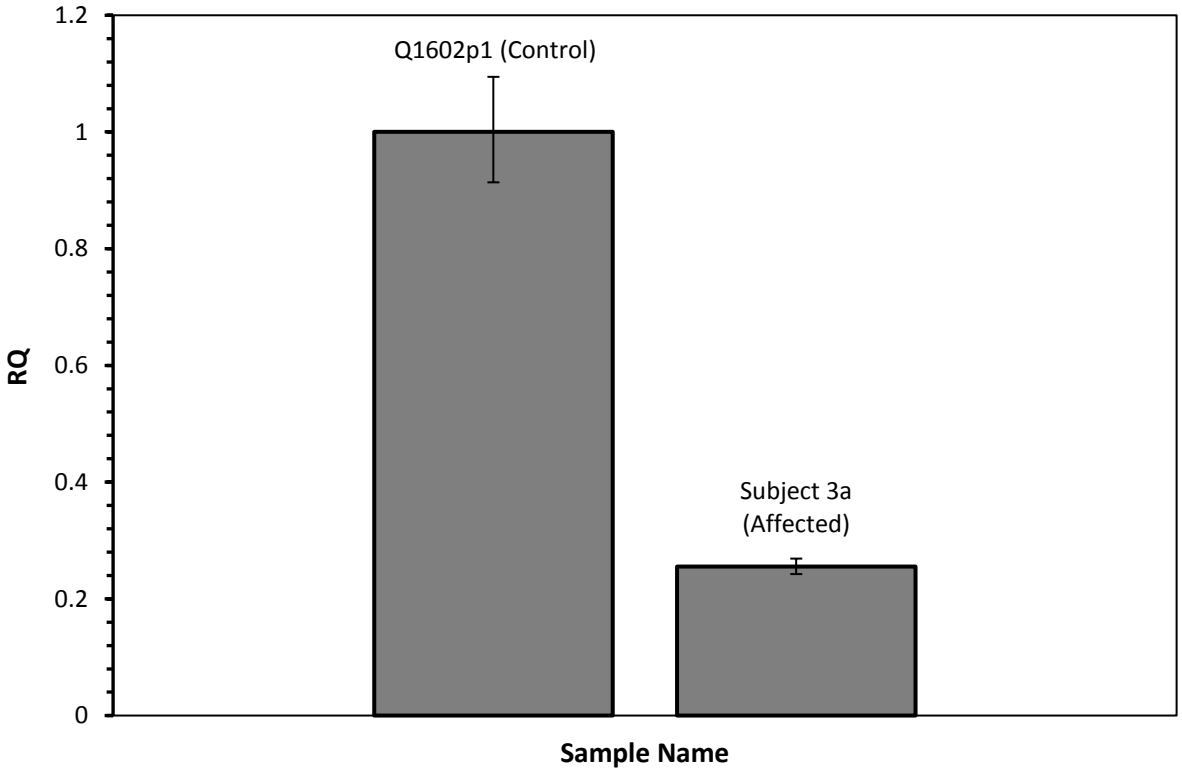

Figure S3. Relative mRNA expression of *MRPS34* in human primary fibroblast cells from subject 3a. Quantitative RT-PCR was performed using a TaqMan probe from Applied Biosystems for *MRPS34* (Hs03043927_m1) and endogenous control gene *ACTB* (Hs01060665g1). $\Delta\Delta C_T$ method was used and data normalized to unaffected control primary fibroblasts (Q1602p1). Data represent 3 technical replicates performed for the subject and 2 control fibroblast cell lines. Error bars represent min/max RQ levels.

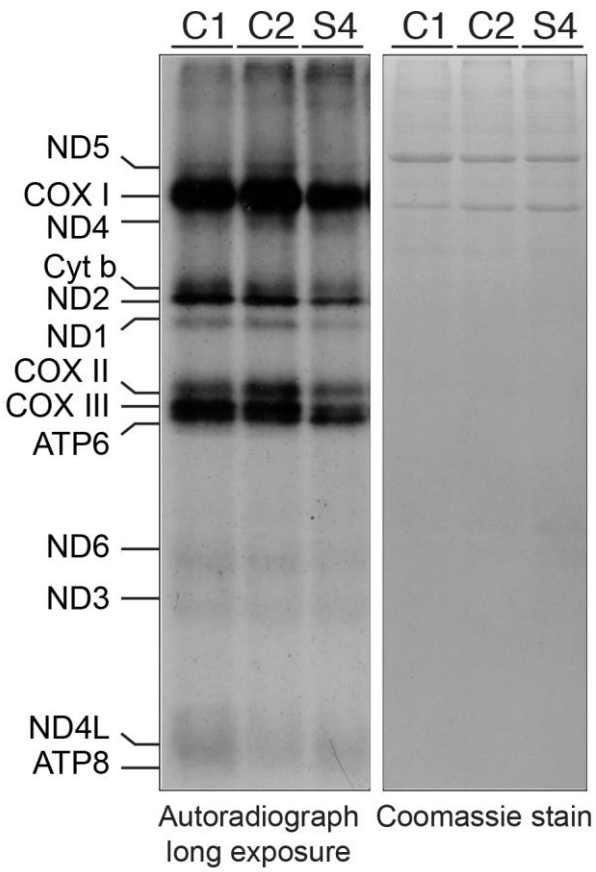

Figure S4. Protein synthesis in cell lysates was measured by pulse incorporation of ^{35}S-labelled methionine and cysteine. Equal amounts of cellular protein were separated by SDS–PAGE and visualized by autoradiography with a long exposure. An image taken following a shorter exposure is shown in Figure 3G. The *in vitro* pulse labelling of mitochondrial translation products revealed decreased levels of mtDNA-encoded subunits in subject 4 relative to controls (C1 and C2). The Coomassie stain represents relative loading.

Table S1. Summary of Clinical Investigations

Individual	**1**	**2a**	**2b**	**3a**	**3b**	**4**
MRPS34 mutation	c.321+1G>T	c.322-10G>A	c.322-10G>A	c.322-10G>A	c.322-10G>A	c.37G>A; c.94C>T
Country of origin	Italy	Puerto Rico	Puerto Rico	Puerto Rico	Puerto Rico	France
Consanguineous	+	-	-	-	-	-
Sex	Male	Female	Female	Female	Female	Male
Age at presentation	4 months	6 months	6 months	6 months	6 months	10 days
Age at last evaluation	4 months	17 years	14 years	7 years	2 years	7 months
Deceased (age)	+ (9 months)	-	-	-	-	+ (8.5 months)
Birth weight	NK	2.55 kg	1.99 kg	3.43 kg	2.3 kg	2.99 kg
Developmental delay	+	+	+	-	+	+
Age at developmental regression	NA	12 months	NA	20 months	NA	4 months
Movement disorder	-	+	+	+	-	Dystonia
Tremor	-	+	-	+	+	-
Epilepsy	-	-	-	-	-	+
Basal ganglia lesions	+	-	-	-	-	+
Brainstem lesions	Normal CT scan at 2 months. At post-mortem symmetrical rarefication of the neuropil, vascular proliferation and gliosis of the tegmentum of the pons, midbrain and basal ganglia	Abnormal bright T2 and FLAIR signal in the posterior half of the midbrain with extension to the quadrigeminal plate. The abnormal signal extends to the posterior portion of the pons, abutting the floor of the 4th ventricle. Small areas of increased T2 and FLAIR signal are seen in both cerebral peduncles at the level of the midbrain (performed at 20 months)	-	Abnormal FLAIR/T2 hyperintensity and restricted diffusion in periaqueductal gray matter (performed at 20 months)	Bilateral symmetric foci of T2 hyperintensity and restricted diffusion in the medulla, restiform bodies, and midbrain	Bilateral abnormal hyperintensities in the brainstem, mainly in the dorsal brainstem nuclei and in periaqueductal region
Cerebellar lesions	-	-	Mild cerebellar atrophy	-	-	-
Thalami lesions	Normal CT scan at 2 months. At post-mortem symmetrical	-	-	Abnormal FLAIR/T2 hyperintensity and restricted diffusion (20	-	-

	rarefication of the neuropil, vascular proliferation and gliosis of the thalami			months); symmetric mild atrophy with gliosis (performed at 5 years)		
MR Spectroscopy	ND	Normal	ND	Normal	Normal	Lactate peak
Dysphagia	-	ND	+	+	+	-
Age at G-tube placement	ND	-	12 years	23 months	ND	-
Constipation	-	+	+	+	-	-
Optic atrophy	-	-	-	+	ND	-
Lactic acidosis	+	+ (mild)	+ (mild)	+ (mild)	+ (mild)	+ (transient)
Muscle pathology	Type 1 fiber predominance and type 2 fiber atrophy. No ragged red fibers were apparent, but double staining with COX/SDH showed a diffuse population of mitochondrial with a COX defect. Similar results were seen with COX/NADH-TR	Left quadriceps: minimal variation in fiber size without fiber type predominance nor architectural disturbances. Normal glycogen and lipd content, no endomysial fibrosis with no vasculitis nor thrombosis.	ND	Randomly dispersed, predominantly type II fiber and to a lesser extent type I fiber atrophy. Patchy increase in subsarcolemmal NADH-TR and COX immunostaining staining	ND	ND
Muscle electron microscopy	ND	ND	ND	Mild increase in subsarcolemmal mitochondria and mitochondria-associated lipid vacuoles	ND	ND
Other	Microcephaly	Scoliosis with surgical intervention; strabismus, s/p corrective surgery; ptosis; horseshoe kidney; microcephaly	Scoliosis with surgical intervention; femur fracture; strabismus, s/p corrective surgery; microcephaly	Precocious adrenarche, slightly advanced bone age	NA	Blindness

NK=not known; ND=not done; NA=not applicable.

Table S2. Oxidative phosphorylation (OXPHOS) enzyme activities.

Subject details	**OXPHOS Activities[a]**				
ID	**Sample Type**	**Enzyme**	**Residual Activity (%)**	**Enzyme Activity**	**Reference Range**
1	Muscle	I	**27**	12	19-90
		II	64	21	16-56
		III	**44**	13	14-67 /min/mg
		IV	**26**	1.4	1.0-10.9 /min/mg
		CS	73	116	76-250
	Liver	I	**28**	4	10-16
		II	147	110	43-100
		III	64	7.9	9-14 /min/mg
		IV	**21**	0.25	0.7-2.2 /min/mg
		CS	209	106	45-56
	Fibroblasts	I	**55**	40	34-141
		II	101	56	22-100
		III	94	12	5-28 /min/mg
		IV	**49**	2.8	1.1-11.6 /min/mg
		CS	157	331	87-322
2a	Muscle (19 months)	I	80	11.82	14.74+/-4.48
		II	117	1.02	0.87+/-0.21
		I+III	90	0.73	0.81+/-0.20
		II+III	72	0.74	1.03+/-0.31
		IV	124	3.02	2.43+/-0.70
		CS	145	22.75	15.74+/-4.44
	Muscle (12 years)	I (n-decyl CoQ)	**49**	42	85 +/-34
		I (CoQ1)	**24**	58	246 +/-118
		I+III	**23**	77	329 +/-198
		II+III	95	386	407 +/- 210
		III	**45**	654	1461 +/-473
		IV	**52**	1243	2388 +/- 916
		CS		357	[b]
2b	Not performed				
3a	Muscle	I+III	**13**	1.2	9.1 +\- 2.5
		II	**29**	2.37	8.11+\-2.44
		II+III	**25**	1.21	4.9 +\- 1.1
		IV	**62**	18.2	29.1 +\- 9.1
		CS	154	432	280+\-95
3b	Not performed				
4	Muscle	I	94	17	10-27
		II	118	39	21-49
		III	89	300	224-476
		IV	**45**	68	91-225
		V	193	145	44-120
		CS	76	79	69-144
	Fibroblasts	I	125	45	28-45
		II	109	75	56-84
		III	92	652	563-882
		IV	**58**	201	274-434
		V	113	76	52-85
		CS	83	183	178-265

[a]Activities of OXPHOS enzyme complexes I, II, III, IV (I, II, III, IV) and citrate synthase (CS) are expressed as % residual activity and as enzyme activity (in nmol/min/mg protein except for complexes III and IV in S1 samples, where results are expressed as first order rate constants relative

to protein). Reference ranges for enzyme activity are shown as observed range or as +/- SD. Bold text represents enzymes regarded as deficient.

[b]MNG Laboratories who performed this testing could not provide a normal range or mean for muscle citrate synthase activity.

Table S3. Principal Component Analysis (PCA) of exome SNP genotypes from families 2 and 3 calculated against representative samples of each of the major 1000 Genomes Project Phase 3 populations plus a GeneDx-sequenced Middle Eastern population. Only SNPs with a population frequency greater than 2% in the 1000 Genome data and located within 20 bps of exons were included for analysis. SNPs on chromosome X and Y were excluded. These filtering steps left 111,638 variants, and any missing calls on the reference list of SNPs in a case sample was replaced with a homozygous reference call. PCA was performed with the R function *prcomp*.[2-4] Ancestry prediction for a case sample was made using k-nearest neighbors method, implemented in the R function *knn*[4,5] on principal components 2 and 3 with k=5. Components are numbered in the order of informativeness and *knn.pred* is the nearest-neighbor-predicted 1000 Genomes super-population.

Individual	**knn.pred**	**PC1**	**PC2**	**PC3**	**PC4**	**PC5**
Family 3, Individual II-1 (S3a)	AMR	1.075177554	-25.69201184	14.36626566	9.4336062	25.91654451
Family 3, Individual I-1	AMR	1.127728779	-22.54695865	15.92007444	7.069130611	23.9091902
Family 2, Individual II-1 (S2a)	AMR	-2.948157115	-23.81871345	20.12656213	1.289456494	44.56063506
Family 2, Individual I-2	AMR	0.631370768	-21.42782257	20.94823352	-1.128908935	42.21331663
Family 2, Individual I-1	AMR	-1.746995075	-24.37604962	18.58769782	6.399003755	35.98355262
Family 2, Individual II-2 (S2b)	AMR	-0.662337519	-23.15999503	17.6338798	2.361260955	44.75422774
Family 3, Individual I-2	AMR	4.483319247	-24.08598252	12.58689777	6.336561635	22.80494419

Table S4. Kinship analysis of families 2 and 3 using whole exome sequencing data, performed as previously described using KING.[6,7]

Individual	**Individual**	**Kinship coefficient**
Family 3, Individual II-1 (S3a)	Family 3, Individual I-1	0.1964
Family 3, Individual II-1 (S3a)	Family 2, Individual II-1 (S2a)	0.0021
Family 3, Individual II-1 (S3a)	Family 2, Individual I-2	0.0083
Family 3, Individual II-1 (S3a)	Family 2, Individual I-1	-0.0255
Family 3, Individual II-1 (S3a)	Family 2, Individual II-2 (S2b)	-0.0122
Family 3, Individual II-1 (S3a)	Family 3, Individual I-2	0.1744
Family 3; Individual I-1	Family 2, Individual II-1 (S2a)	0.0017
Family 3; Individual I-1	Family 2, Individual I-2	-0.0008
Family 3; Individual I-1	Family 2, Individual I-1	-0.0264
Family 3; Individual I-1	Family 2, Individual II-2 (S2b)	-0.0170
Family 3; Individual I-1	Family 3, Individual I-2	-0.0281
Family 2, Individual II-1 (S2a)	Family 2, Individual I-2	0.1986
Family 2, Individual II-1 (S2a)	Family 2, Individual I-1	0.1764
Family 2, Individual II-1 (S2a)	Family 2, Individual II-2 (S2b)	0.1876
Family 2, Individual II-1 (S2a)	Family 3, Individual I-2	-0.0261
Family 2, Individual I-2	Family 2, Individual I-1	-0.0133
Family 2, Individual I-2	Family 2, Individual II-2 (S2b)	0.1897
Family 2, Individual I-2	Family 3, Individual I-2	-0.0151
Family 2, Individual I-1	Family 2, Individual II-2 (S2b)	0.1695
Family 2, Individual I-1	Family 3, Individual I-2	-0.0451
Family 2, Individual II-2 (S2b)	Family 3, Individual I-2	-0.0358

Table S5. Variants in the *MRPS34* genomic region identified by whole exome sequencing in families 2 and 3. Haplotype analysis was performed using high-confidence variant calls that passed clinical pipeline filtering and had a minimum Phred-scaled genotype quality score of 50.

Available as an excel file.

Table S6. Quantitative proteomic data from analysis of fibroblasts from subject 1 and controls. Available as an excel file.

Table S7. Mean level of proteins from each OXPHOS complex and the mitoribosome subunits in subject 1 as a ratio of the control mean. The results of a two-tailed ratio paired t-test are detailed in the table; p-values < 0.00714 were regarded as significant.

List	**Number of proteins quantified by proteomic analysis**	**2-sided p-value**	**Mean of ratios (S1/control mean)**	**95% confidence interval of mean of ratios**
Complex I	38	<0.0001	0.6055	0.5498 to 0.6668
Complex II	4	0.0130	1.274	1.102 to 1.472
Complex III	8	0.0416	0.8594	0.7443 to 0.9924
Complex IV	9	<0.0001	0.5818	0.5144 to 0.6581
Complex V	14	0.8029	0.9863	0.877 to 1.109
Large mitoribosome	46	<0.0001	0.8786	0.8392 to 0.9198
Small mitoribosome	27	<0.0001	0.3624	0.3242 to 0.405

Supplemental references

1. Ballana, E., Govea, N., de Cid, R., Garcia, C., Arribas, C., Rosell, J., and Estivill, X. (2008). Detection of unrecognized low-level mtDNA heteroplasmy may explain the variable phenotypic expressivity of apparently homoplasmic mtDNA mutations. Hum Mutat *29*, 248-257.
2. Becker, R.A., Chambers, J.M., and Wilks, A.R. (1988). The New S Language (Wadsworth & Brooks).
3. Mardia, K.V., Kent, J.T., and Bibby, J.M. (1979). Multivariate Analysis (Academic Press, London).
4. Venerables, W.N., and Ripley, B.D. (2002). Modern Applied Statistics with S (Springer-Verlag New York).
5. Ripley, B.D. (1996). Pattern Recognition and Neural Networks (Cambridge University Press).
6. Retterer, K., Juusola, J., Cho, M.T., Vitazka, P., Millan, F., Gibellini, F., Vertino-Bell, A., Smaoui, N., Neidich, J., Monaghan, K.G., et al. (2016). Clinical application of whole-exome sequencing across clinical indications. Genet Med *18*, 696-704.
7. Manichaikul, A., Mychaleckyj, J.C., Rich, S.S., Daly, K., Sale, M., and Chen, W.M. (2010). Robust relationship inference in genome-wide association studies. Bioinformatics *26*, 2867-2873.